# MESOZOIC AND CENOZOIC SOURCE-ROCK CHARACTERISTICS, PUALE BAY OUTCROPS AND NORTH ALEUTIAN SHELF COST #1 WELL

by
Paul L. Decker[1]

## Abstract

New outcrop geochemical data for Mesozoic source rocks of the Alaska Peninsula are presented alongside similar pre-existing data from Tertiary units of the North Aleutian basin, facilitating direct comparison of key characteristics that determine the type and quantity of expelled petroleum. Consisting of total organic carbon, Rock-Eval pyrolysis, kerogen petrography, and vitrinite reflectance data from samples of Triassic Kamishak and Jurassic Kialagvik Formation exposures at Puale Bay, the new data confirm previous descriptions of these source-rock units as highly oil-prone. More importantly, this dataset establishes important distinctions between the two Mesozoic formations, and provides constraints on the stratigraphic variations and lithofacies associations of the quantity and type of organic matter within each unit. Additionally, the Puale Bay vitrinite reflectance data are the first to confirm the section's immature to early oil-window thermal maturity previously indicated only by pyrolysis data. The same approach applied to Tertiary formations penetrated in the North Aleutian Shelf COST #1 well and a small population of outcrop coal samples provides details supporting the conclusion reached by previous workers that the Cenozoic backarc basin fill is dominated by terrestrially-sourced coaly kerogen, and is most prospective for natural gas. Though certain facies may possess marginal capability to generate petroleum liquids, particularly carbonaceous mudstones within the Tolstoi Formation and some coals of the Bear Lake Formation, high matrix adsorption effects are likely to limit expulsion efficiency, minimizing the likelihood of significant Tertiary-sourced oil accumulations in the basin.

## INTRODUCTION

The Alaska Peninsula hosts potential petroleum systems of both Mesozoic and Cenozoic age (Finzel and others, 2005; Sherwood and others, 2006; Decker and others, 2006; Reifenstuhl and others, 2007), but to date neither has yielded commercial production. A significant difference between these two petroleum systems is that source rocks of the Mesozoic system contain dominantly oil-prone marine organic matter (Wang and others, 1988; Magoon and Anders, 1992), whereas those of the Cenozoic system are dominated by gas-prone terrestrial kerogens (Dow, 1983; Turner and others, 1988; Sherwood and others, 2006).

On the southeastern side of the northern Alaska Peninsula near Wide Bay, Becharof Lake, and Puale Bay, surface petroleum seeps leave no doubt that the Mesozoic petroleum system contains effective oil and gas source rocks. At least 14 historically active seeps of oil or flammable gas in this area have been catalogued by Blodgett and Clautice (2005) as emanating from Jurassic rocks of the Chignik subterrane, the southeastern block of the Alaska Peninsula terrane (fig. 1; Wilson and others, 1985, 1999). Magoon and Anders (1990, 1992) presented biomarker and isotopic evidence linking these seeps to the underlying Upper Triassic Kamishak Formation and the mostly Middle Jurassic Kialagvik Formations (fig. 2). Age-equivalent source-rock units extend northeastward beneath much of the Cook Inlet basin, where the Middle Jurassic Tuxedni Group is the principal source of oil in commercial fields in upper Cook Inlet, and Upper Triassic strata contribute to non-commercial oil occurrences in lower Cook Inlet (Magoon and Claypool, 1981; Magoon and Anders, 1990, 1992; Magoon, 1994).

In contrast, the Quaternary-covered northwestern side of the northern Alaska Peninsula (Bristol Bay Lowlands area) is devoid of active hydrocarbon seeps. There, in the northeast portion of the North Aleutian basin, the three wells that penetrate the full Cenozoic sedimentary and volcanic section of the Ugashik subbasin (fig. 1; Decker, Reifenstuhl and Gillis, this volume) are interpreted to pass directly into Mesozoic igneous and metamorphic basement of the Iliamna subterrane of the Alaska Peninsula terrane (Wilson and others, 1985; 1999), without encountering source-prone Mesozoic sedimentary rocks.

On the southwestern Alaska Peninsula southwest of Port Moller, Chignik subterrane units are uplifted and exposed along the southern margin of the main North Aleutian basin. Thermogenic natural gas seeps vigorously from fractured Cretaceous Herendeen Formation at the Port Moller hot spring (Decker and others, 2005), most likely derived from an underlying Mesozoic source. Minor oil shows occur in Tertiary strata in several wells within and along this edge of the North Aleutian basin, but Sherwood and others (2006) consider it unlikely that

[1]Alaska Division of Oil & Gas, 550 W. 7th Ave., Suite 800, Anchorage, Alaska 99501

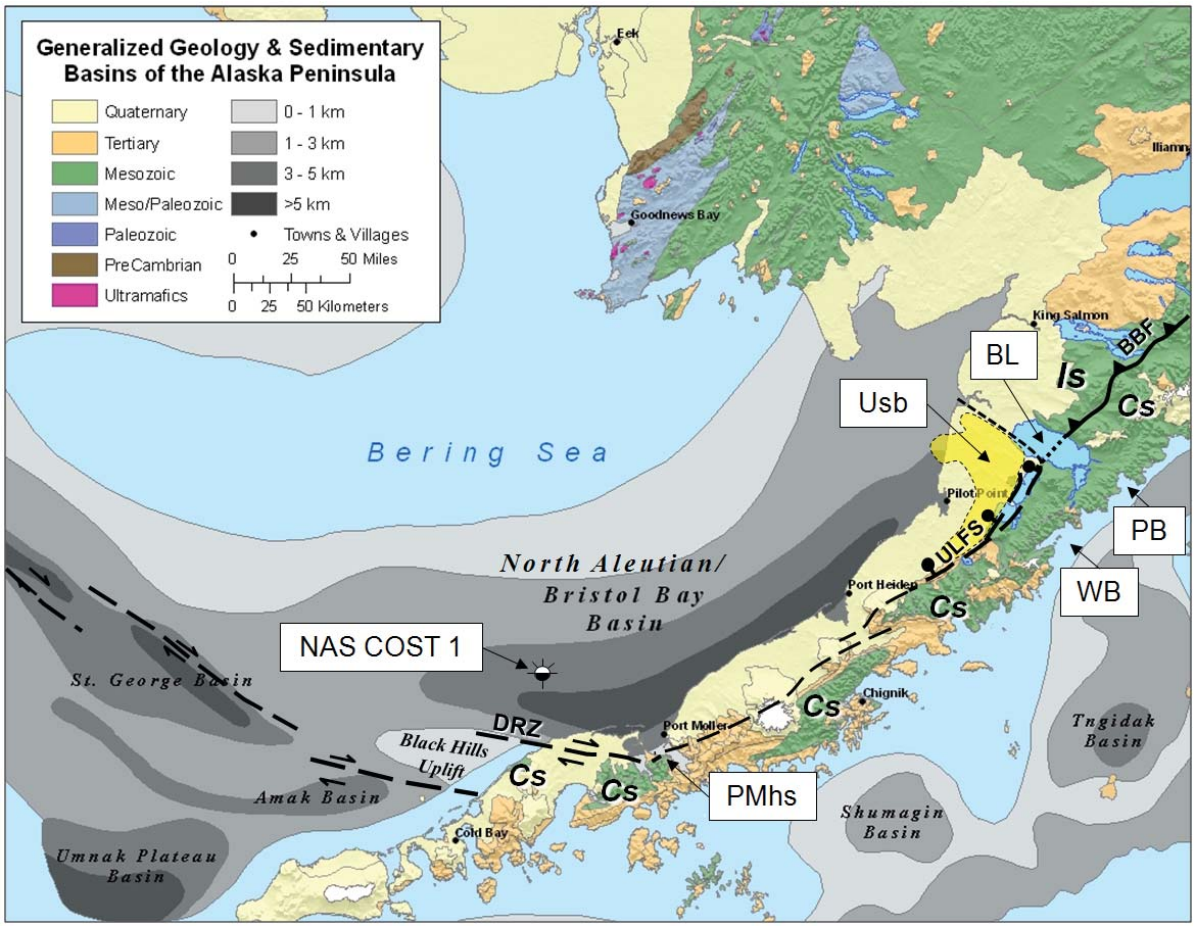


*Figure 1. Location map of the Alaska Peninsula showing generalized geologic units, tectonic elements, and localities referred to in text. Abbreviations as follows: PB = Puale Bay, WB = Wide Bay, BL = Becharof Lake, Usb = Ugashik sub-basin, PMhs = Port Moller hot spring (gas seep), Cs =Chignik sub-terrane (in places covered by Cenozoic overlap succession), Is = Iliamna sub-terrane, BBF = Bruin Bay fault, ULFS = Ugashik Lakes fault system, DRZ = David River zone. Geologic age units after Beikman (1980); basin isopachs from Kirschner (1988).*

oil-prone Chignik subterrane source-rock units underlie substantial areas of the basin offshore, and view the coaly nonmarine to shallow marine Tertiary section there as primarily prospective for natural gas.

This report presents recently obtained total organic carbon, Rock-Eval pyrolysis, organic petrography, and vitrinite reflectance ($R_o$) thermal maturity data from outcrops of the Triassic Kamishak and Jurassic Kialagvik formations at Puale Bay (table 1, These data are used to describe their petroleum source-rock characteristics and to draw figs. 3–5).contrasts between them and the Tertiary formations of the North Aleutian basin, mainly as documented using data from the North Aleutian Shelf COST #1 well (fig. 1; Dow, 1983; Turner and others, 1988; Sherwood and others, 2006). This study is neither a comprehensive overview of regional source rock geochemistry nor an exhaustive compilation or treatment of all the relevant data that might be assembled from a variety of sources. It is intended to present new outcrop data in the context of existing data, and to provide insight into the fundamental differences between the Mesozoic and Cenozoic petroleum systems noted above.

## SOURCE-ROCK EVALUATION APPROACH

The data considered here address the fundamental parameters required to describe a rock's potential and effectiveness as a petroleum source: (1) the quantity or richness of organic matter, (2) the quality or type of organic matter, and (3) the thermal maturity or extent of heating (Tissot and Welte, 1984; Peters and Cassa, 1994). The following overview introduces many of the terms and concepts used in source-rock characterization. Key references for further reading on analytical procedures, applications, and pitfalls of these techniques include Espitalie and others (1977, 1985), Dow (1977), Tissot and Welte (1984), Peters (1986), Langford and Blanc-Valleron (1990), and Peters and Cassa (1994).

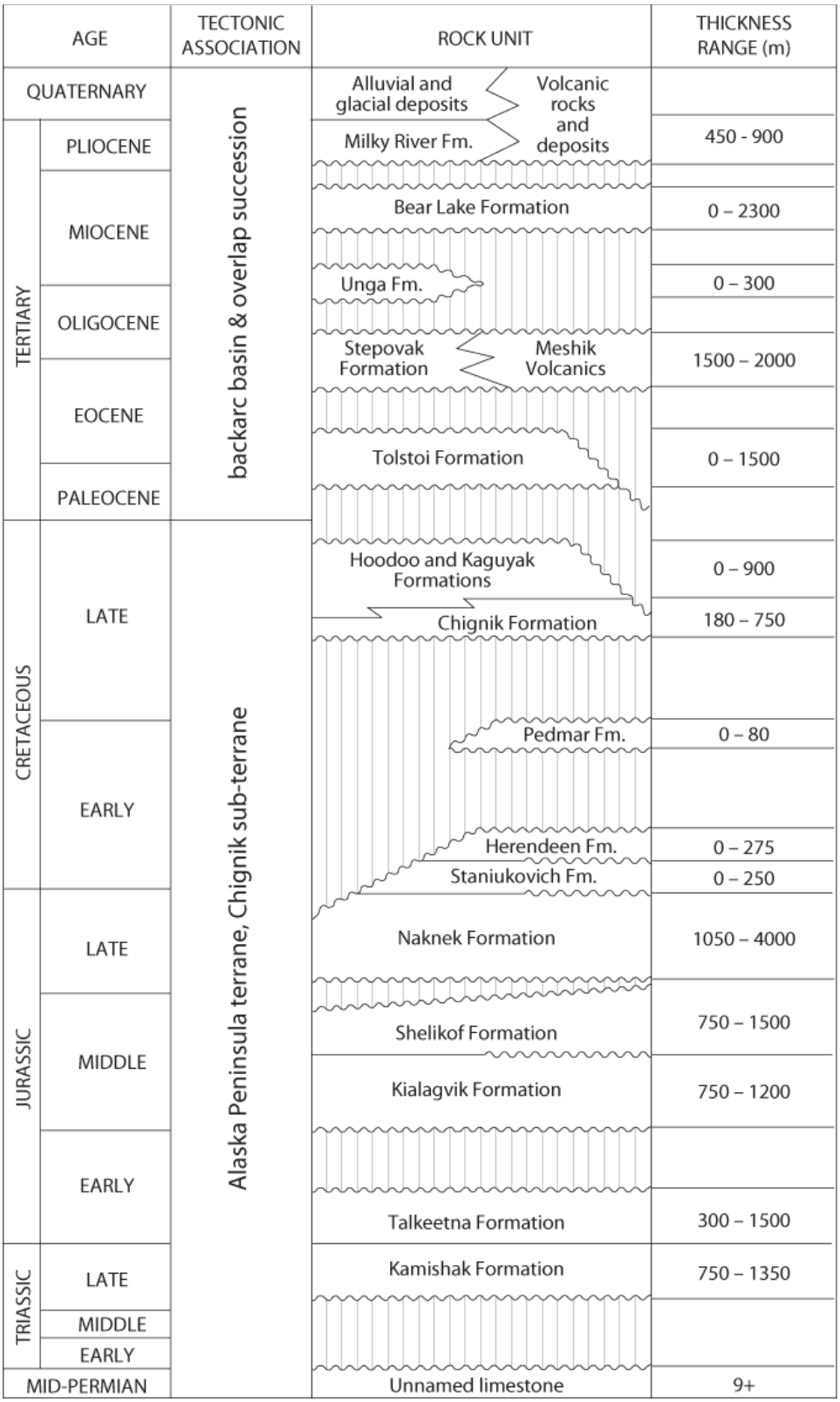


*Figure 2. Composite stratigraphic column for the Alaska Peninsula, modified after Beeman and others (1996) and Detterman and others (1996). Metamorphic and plutonic units, including the Iliamna sub-terrane of the Alaska Peninsula terrane, are not depicted.*

*Table 1. Total organic carbon, Rock-Eval pyrolysis, mean vitrinite reflectance, and kerogen compositional analysis data for Kamishak and Kialagvik Formation samples collected at Puale Bay 2004–2007.*

| Field Sample ID | Formation | Latitude | Longitude | Comments | TOC Wt. % | S1 mg/g | S2 mg/g | S3 mg/g | Tmax | HI | OI | S1/ TOC | PI | %Ro Mean | %Liptinite | %Vitrinite | %Inert |
|---|---|---|---|---|---|---|---|---|---|---|---|---|---|---|---|---|---|
| 04RR011A | Kialagvik Formation | -- | -- | outcrop | 0.81 | 0.30 | 0.58 | 0.32 | 444 | 72 | 40 | 37 | 0.34 | - | - | - | - |
| 04RR011B | Kialagvik Formation | -- | -- | outcrop | 0.57 | 0.09 | 0.33 | 0.28 | 465 | 58 | 49 | 16 | 0.21 | - | - | - | - |
| 04TJR008 | Kialagvik Formation | -- | -- | outcrop | 0.54 | 0.08 | 0.33 | 0.13 | 461 | 61 | 24 | 15 | 0.19 | - | - | - | - |
| 05EF100 | Kialagvik Formation | 57.73653 | -155.39818 | outcrop | 0.71 | 0.13 | 1.15 | 0.55 | 425 | 162 | 77 | 18 | 0.10 | - | - | - | - |
| 05EF101 | Kialagvik Formation | 57.73612 | -155.39775 | outcrop | 2.79 | 0.77 | 18.94 | 0.67 | 425 | 680 | 24 | 28 | 0.04 | - | - | - | - |
| 05EF102 | Kialagvik Formation | 57.73528 | -155.39732 | outcrop | 1.22 | 0.18 | 4.44 | 0.60 | 428 | 364 | 49 | 15 | 0.04 | - | - | - | - |
| 05EF103 | Kialagvik Formation | 57.73480 | -155.39700 | outcrop | 1.92 | 0.47 | 10.64 | 0.64 | 429 | 554 | 33 | 24 | 0.04 | - | - | - | - |
| 05RR208 | Kialagvik Formation | 57.73674 | -155.40101 | outcrop | 3.51 | 0.89 | 22.12 | 0.67 | 423 | 630 | 19 | 25 | 0.04 | - | - | - | - |
| 05RR209A | Kialagvik Formation | 57.73786 | -155.40276 | outcrop | 0.81 | 0.13 | 1.94 | 0.49 | 425 | 240 | 60 | 16 | 0.06 | - | - | - | - |
| 05RR210A | Kialagvik Formation | 57.73909 | -155.40446 | outcrop | 1.46 | 0.22 | 4.56 | 0.38 | 424 | 312 | 26 | 15 | 0.05 | - | - | - | - |
| 05RR210B | Kialagvik Formation | 57.73909 | -155.40446 | o/crop coal | 48.13 | 3.22 | 67.55 | 3.96 | 417 | 140 | 8 | 7 | 0.05 | - | - | - | - |
| 07BG225A | Kialagvik Formation | 57.73354 | -155.39645 | outcrop | 1.97 | 0.46 | 11.16 | 0.28 | 431 | 566 | 14 | 23 | 0.04 | 0.52 | 95 | 5 | 0 |
| 07BG226A | Kialagvik Formation | 57.73426 | -155.39670 | outcrop | 1.55 | 0.36 | 6.58 | 0.28 | 430 | 423 | 18 | 23 | 0.05 | 0.50 | 95 | 5 | 0 |
| 07BG227A | Kialagvik Formation | 57.73426 | -155.39716 | outcrop | 1.57 | 0.33 | 6.75 | 0.34 | 435 | 429 | 22 | 21 | 0.05 | 0.52 | 95 | 5 | 0 |
| 07BG228A | Kialagvik Formation | 57.73526 | -155.39738 | outcrop | 1.86 | 0.38 | 8.14 | 0.31 | 435 | 438 | 17 | 21 | 0.04 | 0.50 | 90 | 10 | 0 |
| 07BG229A | Kialagvik Formation | 57.73602 | -155.39789 | outcrop | 1.57 | 0.39 | 7.31 | 0.34 | 434 | 466 | 22 | 25 | 0.05 | 0.53 | 95 | 5 | 0 |
| 07BG230A | Kialagvik Formation | 57.73652 | -155.39825 | outcrop | 1.84 | 0.48 | 10.31 | 0.29 | 431 | 562 | 16 | 26 | 0.04 | 0.56 | 95 | 5 | 0 |
| 07BG231A | Kialagvik Formation | 57.73785 | -155.39960 | outcrop | 1.16 | 0.16 | 3.48 | 0.23 | 434 | 300 | 20 | 13 | 0.04 | 0.51 | 95 | 5 | 0 |
| 07BG232A | Kialagvik Formation | 57.73872 | -155.40105 | outcrop | 0.96 | 0.14 | 2.29 | 0.24 | 431 | 240 | 25 | 14 | 0.06 | 0.52 | 95 | 5 | 0 |
| 07BG233A | Kialagvik Formation | 57.73967 | -155.40247 | outcrop | 0.97 | 0.13 | 2.64 | 0.24 | 434 | 273 | 25 | 13 | 0.05 | 0.54 | 95 | 5 | 0 |
| 07PD183A | Kialagvik Formation | 57.74152 | -155.40685 | outcrop | 0.54 | 0.07 | 0.71 | 0.29 | 429 | 131 | 53 | 13 | 0.09 | 0.52 | 30 | 65 | 5 |
| 07PD183B | Kialagvik Formation | 57.74152 | -155.40685 | o/crop coal | 69.50 | 1.34 | 148.52 | 2.41 | 421 | 214 | 3 | 2 | 0.01 | 0.71 | 5 | 90 | 5 |
| 07PD184A | Kialagvik Formation | 57.74243 | -155.40843 | outcrop | 0.99 | 0.07 | 1.12 | 0.17 | 436 | 114 | 17 | 7 | 0.06 | 0.59 | 30 | 65 | 5 |
| 07PD185A | Kialagvik Formation | 57.74352 | -155.41051 | outcrop | 0.97 | 0.05 | 1.11 | 0.15 | 435 | 114 | 16 | 5 | 0.04 | 0.52 | 20 | 75 | 5 |
| 07PD186A | Kialagvik Formation | 57.74524 | -155.41440 | outcrop | 0.79 | 0.03 | 1.05 | 0.15 | 431 | 132 | 19 | 4 | 0.03 | 0.53 | 40 | 55 | 5 |
| 07PD187A | Kialagvik Formation | 57.74581 | -155.41609 | outcrop | 0.60 | 0.07 | 0.81 | 0.22 | 429 | 136 | 37 | 12 | 0.08 | 0.54 | 40 | 55 | 5 |
| 07PD188A | Kialagvik Formation | 57.74665 | -155.41891 | outcrop | 0.44 | 0.03 | 0.26 | 0.21 | 430 | 59 | 48 | 7 | 0.10 | 0.49 | 25 | 70 | 5 |
| 07RR027A | Kialagvik Formation | 57.74744 | -155.43813 | outcrop | 0.35 | 0.02 | 0.10 | 0.60 | 443 | 29 | 171 | 6 | 0.16 | 0.53 | 70 | 25 | 5 |
| 07RR028A | Kialagvik Formation | 57.74748 | -155.43777 | outcrop | 0.16 | 0.01 | 0.09 | 0.28 | 447 | 58 | 179 | 6 | 0.10 | 0.53 | 95 | 5 | 0 |
| 07RR029A | Kialagvik Formation | 57.74731 | -155.43799 | outcrop | 0.45 | 0.02 | 0.43 | 0.37 | 426 | 96 | 82 | 4 | 0.04 | 0.52 | 95 | 5 | 0 |
| 07RR030A | Kialagvik Formation | 57.74726 | -155.43791 | outcrop | 0.32 | 0.03 | 0.19 | 0.27 | 425 | 60 | 86 | 10 | 0.14 | 0.55 | 95 | 5 | 0 |
| 07RR031A | Kialagvik Formation | 57.74720 | -155.43796 | outcrop | 1.48 | 0.08 | 3.14 | 0.66 | 429 | 213 | 45 | 5 | 0.02 | 0.55 | 95 | 5 | 0 |
| 07RR032A | Kialagvik Formation | 57.74723 | -155.43805 | outcrop | 0.99 | 0.05 | 1.28 | 0.65 | 433 | 129 | 66 | 5 | 0.04 | 0.44 | 95 | 5 | 0 |
| 07RR033A | Kialagvik Formation | 57.74726 | -155.43782 | outcrop | 0.59 | 0.02 | 0.46 | 0.39 | 431 | 78 | 67 | 3 | 0.04 | 0.57 | 95 | 5 | 0 |
| 07RR034A | Kialagvik Formation | 57.74715 | -155.43790 | outcrop | 1.89 | 0.11 | 5.08 | 0.71 | 428 | 269 | 38 | 6 | 0.02 | 0.50 | 95 | 5 | 0 |
| 07RR035A | Kialagvik Formation | 57.74706 | -155.43784 | outcrop | 0.17 | 0.03 | 0.13 | 0.22 | 442 | 76 | 128 | 17 | 0.18 | 0.56 | 95 | 5 | 0 |
| 07RR036A | Kialagvik Formation | 57.74704 | -155.43788 | outcrop | 0.18 | 0.03 | 0.06 | 0.26 | 376 | 33 | 144 | 16 | 0.33 | 0.62 | 90 | 5 | 5 |
| 07RR037A | Kialagvik Formation | 57.74696 | -155.43745 | outcrop | 0.11 | 0.01 | 0.04 | 0.25 | 433 | 37 | 234 | 9 | 0.20 | 0.59 | 90 | 5 | 5 |
| 07RR038A | Kialagvik Formation | 57.74687 | -155.43622 | outcrop | 0.48 | 0.02 | 0.40 | 0.16 | 431 | 84 | 34 | 4 | 0.05 | 0.57 | 85 | 10 | 5 |
| | **Kialagvik averages (excluding coals)** | | | | **1.06** | **0.18** | **3.79** | **0.36** | **432** | **235** | **55** | **14** | **0.09** | **0.53** | **79** | **19** | **2** |

*Table 1. Total organic carbon, Rock-Eval pyrolysis, mean vitrinite reflectance, and kerogen compositional analysis data for Kamishak and Kialagvik Formation samples collected at Puale Bay 2004–2007—continued.*

| Field Sample ID | Formation | Latitude | Longitude | Comments | TOC Wt. % | S1 mg/g | S2 mg/g | S3 mg/g | Tmax | HI | OI | S1/ TOC | PI | Ro Mean | %Liptinite | %Vitrinite | %Inert |
|---|---|---|---|---|---|---|---|---|---|---|---|---|---|---|---|---|---|
| 04DS013A | Kamishak Formation | -- | -- | outcrop | 2.38 | 1.28 | 14.24 | 0.50 | 429 | 598 | 21 | 54 | 0.08 | - | - | - | - |
| 04DS014 | Kamishak Formation | -- | -- | outcrop | 1.12 | 0.33 | 5.31 | 0.25 | 425 | 474 | 22 | 30 | 0.06 | - | - | - | - |
| 05EF104 | Kamishak Formation | 51.71673 | -155.36079 | outcrop | 0.04 | 0.02 | 0.04 | 0.26 | 458 | 100 | 650 | 50 | 0.34 | - | - | - | - |
| 05EF105 | Kamishak Formation | 57.71724 | -155.36040 | outcrop | 0.53 | 0.08 | 0.71 | 0.35 | 429 | 134 | 66 | 15 | 0.10 | - | - | - | - |
| 05RR211A | Kamishak Formation | 57.71422 | -155.36311 | outcrop | 1.01 | 0.15 | 2.39 | 0.72 | 428 | 237 | 71 | 15 | 0.06 | - | - | - | - |
| 05RR212A | Kamishak Formation | 57.71674 | -155.36099 | outcrop | 0.29 | 0.07 | 0.35 | 0.55 | 424 | 121 | 190 | 23 | 0.16 | - | - | - | - |
| 05RR213A | Kamishak Formation | 57.71677 | -155.36170 | outcrop | 0.75 | 0.14 | 1.68 | 0.51 | 426 | 224 | 68 | 19 | 0.08 | - | - | - | - |
| 07BG237A | Kamishak Formation | 57.71453 | -155.36455 | outcrop | 1.85 | 1.04 | 9.60 | 0.48 | 435 | 519 | 26 | 56 | 0.10 | 0.53 | 95 | 5 | 0 |
| 07BG238A | Kamishak Formation | 57.71367 | -155.36200 | outcrop | 0.07 | 0.04 | 0.17 | 0.27 | 439 | 250 | 395 | 56 | 0.18 | 0.68 | 70 | 25 | 5 |
| 07BG239A | Kamishak Formation | 57.71445 | -155.36302 | outcrop | 0.60 | 0.16 | 1.23 | 0.34 | 433 | 206 | 57 | 27 | 0.11 | 0.86 | 70 | 25 | 5 |
| 07MW003-44.6 | Kamishak Formation | app. 57.71887 | -155.38973 | outcrop | 0.26 | 0.02 | 0.32 | 0.29 | 431 | 125 | 113 | 8 | 0.06 | - | - | - | - |
| 07MW003-54.4 | Kamishak Formation | app. 57.71887 | -155.38973 | outcrop | 0.14 | 0.01 | 0.11 | 0.22 | 425 | 77 | 154 | 7 | 0.08 | - | - | - | - |
| 07MW004-3.2 | Kamishak Formation | app. 57.72031 | -155.38978 | outcrop | 1.22 | 0.33 | 5.34 | 0.26 | 432 | 437 | 21 | 27 | 0.06 | - | - | - | - |
| 07MW005-43.0 | Kamishak Formation | app. 57.71372 | -155.36167 | outcrop | 0.29 | 0.07 | 0.43 | 0.24 | 433 | 150 | 84 | 23 | 0.14 | - | - | - | - |
| 07PD181A | Kamishak Formation | 57.71844 | -155.39035 | outcrop | 3.40 | 1.97 | 26.69 | 0.39 | 434 | 785 | 11 | 58 | 0.07 | 0.54 | 95 | 5 | 0 |
| 07PD182A | Kamishak Formation | 57.71819 | -155.39078 | outcrop | 2.95 | 1.72 | 22.05 | 0.42 | 434 | 746 | 14 | 58 | 0.07 | 0.62 | 95 | 5 | 0 |
| 07PD191A | Kamishak Formation | 57.71493 | -155.36719 | outcrop | 2.51 | 1.36 | 15.33 | 0.46 | 436 | 611 | 18 | 54 | 0.08 | 0.52 | 95 | 5 | 0 |
| 07PD191B | Kamishak Formation | 57.71493 | -155.36719 | outcrop | 2.53 | 1.60 | 15.27 | 0.46 | 433 | 604 | 18 | 63 | 0.09 | 0.54 | 95 | 5 | 0 |
| 07PD192A | Kamishak Formation | 57.71499 | -155.36575 | outcrop | 1.20 | 0.34 | 5.41 | 0.29 | 434 | 450 | 24 | 28 | 0.06 | 0.62 | 95 | 5 | 0 |
| 07PD193A | Kamishak Formation | 57.71367 | -155.36200 | outcrop | 0.09 | 0.02 | 0.18 | 0.25 | 442 | 207 | 285 | 22 | 0.10 | 0.72 | 65 | 5 | 30 |
| 07PD194A | Kamishak Formation | 57.71370 | -155.36179 | outcrop | 0.10 | 0.01 | 0.05 | 0.22 | 469 | 50 | 221 | 10 | 0.16 | 0.61 | 55 | 15 | 30 |
| 07PD195A | Kamishak Formation | 57.72574 | -155.33485 | outcrop | 2.41 | 0.73 | 8.12 | 0.37 | 436 | 337 | 15 | 30 | 0.08 | 0.65 | 90 | 5 | 5 |
| 07PD196A | Kamishak Formation | 57.72586 | -155.33530 | outcrop | 2.98 | 0.93 | 21.22 | 0.32 | 435 | 713 | 11 | 31 | 0.04 | 0.60 | 90 | 5 | 5 |
| 07PD198A | Kamishak Formation | 57.72554 | -155.33755 | outcrop | 5.28 | 3.23 | 39.87 | 0.41 | 440 | 756 | 8 | 61 | 0.07 | 0.52 | 90 | 5 | 5 |
| 07PD199A | Kamishak Formation | 57.72556 | -155.33821 | outcrop | 4.83 | 2.10 | 36.55 | 0.51 | 436 | 756 | 11 | 43 | 0.05 | 0.43 | 90 | 5 | 5 |
| 07PD199B | Kamishak Formation | 57.72556 | -155.33821 | outcrop | 1.74 | 0.76 | 12.54 | 0.48 | 439 | 720 | 27 | 43 | 0.06 | 0.50 | 90 | 5 | 5 |
| 07RB013C | Kamishak Formation | -- | -- | outcrop | - | - | - | - | - | - | - | - | - | 0.70 | 80 | 5 | 15 |
| 07RB04 | Kamishak Formation | app. 57.71887 | -155.38973 | outcrop | 1.32 | 0.32 | 5.62 | 0.26 | 433 | 425 | 20 | 24 | 0.05 | - | - | - | - |
| 07RB05 | Kamishak Formation | app. 57.71887 | -155.38973 | outcrop | 0.62 | 0.17 | 1.79 | 0.27 | 436 | 290 | 44 | 27 | 0.09 | - | - | - | - |
| 07RB06 | Kamishak Formation | app. 57.71887 | -155.38973 | outcrop | 1.81 | 0.20 | 3.64 | 0.18 | 433 | 201 | 10 | 11 | 0.05 | - | - | - | - |
| 07RB07 | Kamishak Formation | app. 57.71887 | -155.38973 | outcrop | 1.08 | 0.18 | 3.39 | 0.22 | 434 | 314 | 20 | 16 | 0.05 | - | - | - | - |
| 07RB11 | Kamishak Formation | app. 57.71378 | 155.36187 | outcrop | 0.12 | 0.01 | 0.09 | 0.29 | 433 | 76 | 244 | 8 | 0.10 | - | - | - | - |
| 07RR041A | Kamishak Formation | 57.71477 | -155.36534 | outcrop | 2.13 | 1.07 | 12.55 | 0.40 | 435 | 589 | 19 | 50 | 0.08 | 0.51 | 85 | 10 | 5 |
| 07RR042A | Kamishak Formation | 57.71412 | -155.36342 | outcrop | 0.44 | 0.12 | 0.78 | 0.27 | 429 | 176 | 61 | 26 | 0.13 | 0.67 | 80 | 10 | 10 |
| 07RR043A | Kamishak Formation | 57.72483 | -155.34138 | outcrop | 0.04 | 0.01 | 0.08 | 0.29 | 460 | 222 | 806 | 27 | 0.11 | 0.64 | 95 | 5 | 0 |
| 07RR044A | Kamishak Formation | 57.72551 | -155.34152 | outcrop | 0.07 | 0.02 | 0.07 | 0.33 | 435 | 97 | 458 | 27 | 0.22 | 0.65 | 85 | 10 | 5 |
| 07RR045A | Kamishak Formation | 57.72523 | -155.34200 | outcrop | 0.43 | 0.10 | 0.85 | 0.50 | 432 | 196 | 115 | 24 | 0.11 | 0.64 | 80 | 15 | 5 |
| 07RR046A | Kamishak Formation | 57.72499 | -155.34346 | outcrop | 1.20 | 0.54 | 3.98 | 0.22 | 431 | 331 | 18 | 45 | 0.12 | 0.51 | 80 | 10 | 10 |
| 07RR047A | Kamishak Formation | 57.72488 | -155.34433 | outcrop | 2.06 | 0.56 | 7.25 | 0.69 | 430 | 352 | 33 | 27 | 0.07 | 0.48 | 90 | 5 | 5 |
| | **Kamishak averages** | | | | **1.37** | **0.57** | **7.51** | **0.36** | **435** | **359** | **117** | **32** | **0.10** | **0.60** | **85** | **8** | **7** |

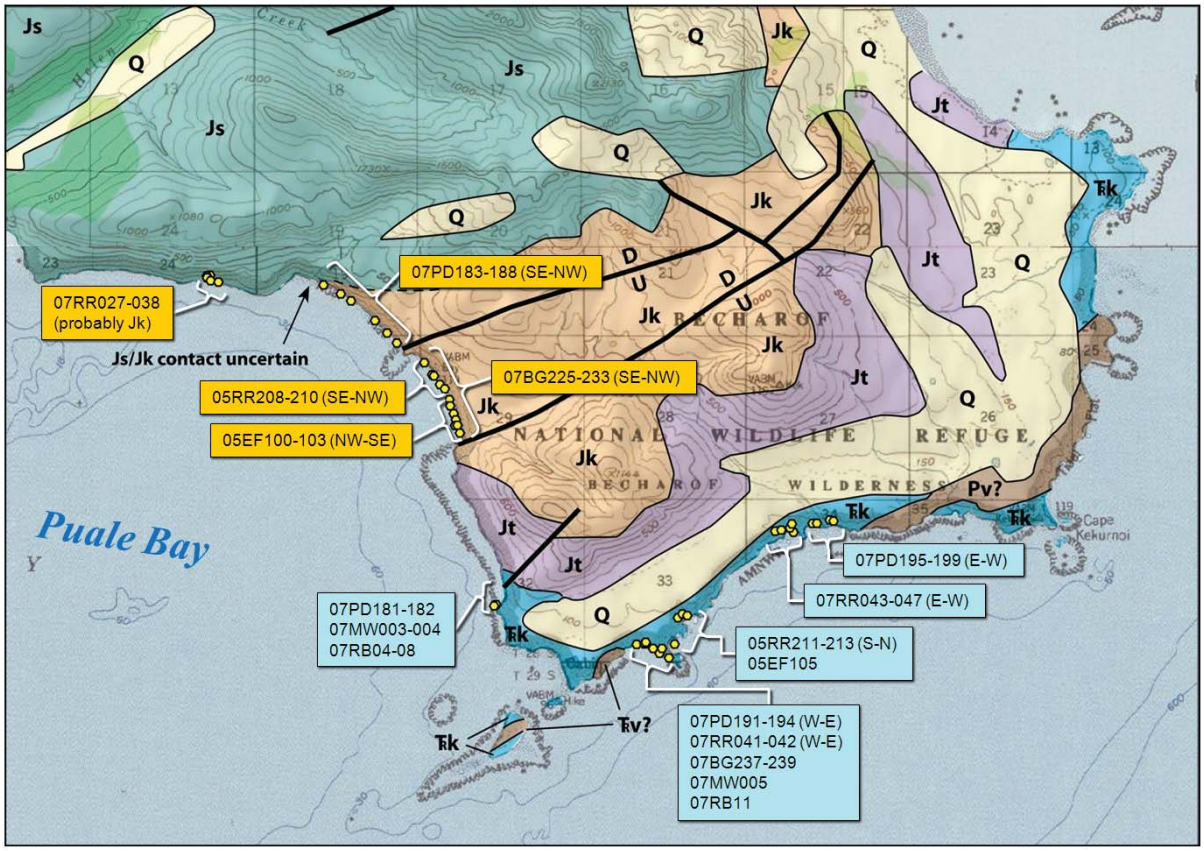


*Figure 3. Simplified geology of Puale Bay exposures referred to in text showing location of source rock sampling stations in the Kamishak Formation (blue labels) and Kialagvik Formation (orange labels). Mapping adapted from USGS maps (Detterman and others, 1987; Wilson and others, 1999); some labels modified to reflect uncertainties described in text. Map units as follows: Pv? = Permian(?) volcanic breccia unconformably underlying Triassic Kamishak Formation; Trv? = Triassic(?) volcanic breccia (note that both Pv? and Trv? were mapped by USGS as Trv); Trk = Kamishak Formation; Jt = Talkeetna Formation; Jk = Kialagvik Formation; Js = Shelikof Formation; Q = Quaternary, undifferentiated. Js/Jk contact can arguably be placed farther north, immediately overlying the farthest northwest samples, here considered to be from the uppermost part of the Kialagvik Formation.*

The quantity of organic matter in a source rock is expressed simply as total organic carbon (TOC) as a percentage of the total sample weight. TOC varies from approximately 0.5 percent in lean source rocks to more than 50 percent in true coals (for example, Peters and Cassa, 1994). Many good to excellent source shales fall in the 1–5 percent range, and carbonaceous shales, siltstones, and other coaly lithologies span the range of TOC up to 50 percent. Modern geochemical laboratories quantify TOC using standardized combustion equipment and techniques.

It is essential to understand the types of kerogen that constitute the organic content because some kerogens are rich enough in hydrogen that they can generate both oil and gas (Types I, II, and II–III mixtures), whereas others contain limited hydrogen and are capable of generating mainly gas (Type III), and others are essentially inert (Type IV). A source rock's kerogen makeup depends mainly on its depositional environment, which determines both the types of kerogen that are present and their preservation potential. Ideally, kerogen typing should be carried out using complementary techniques, such as optical microscopy examination of the kerogen macerals and elemental analysis to quantify atomic H/C (hydrogen/carbon) and O/C (oxygen/carbon) ratios (Tissot and Welte, 1984). These atomic ratios are used to construct traditional van Krevelen diagrams, which, at low thermal maturity, clearly distinguish between hydrogen-rich and hydrogen-poor source rocks. At higher maturity levels, the kerogen type fields converge and overlap due to the progressive depletion of hydrogen and oxygen. The importance of controlling for thermal maturity in source-rock characterization is discussed further in subsequent paragraphs.

For practical reasons, screening studies routinely use efficient but less definitive methods to assess kero-

gen type. One widely employed technique uses TOC in conjunction with the results of Rock-Eval pyrolysis (Espitalie and others, 1977, 1985) to construct a pseudo- or modified van Krevelen diagram. Rock-Eval is a controlled heating procedure that quantifies the amounts of pre-existing volatile hydrocarbon (S1), pyrolyzable hydrocarbon (S2), and carbon dioxide (S3) released from the rock sample over specific temperature ranges. Two key parameters determined by these measurements are hydrogen index (HI=S2/TOC x 100) and oxygen index (OI=S3/TOC x 100), which are typically plotted as proxies for atomic ratios on a modified van Krevelen diagram to distinguish kerogen types. As with true van Krevelen diagrams, the distinction between kerogen types on this sort of plot is greatest in thermally immature samples, and the fields overlap considerably at higher maturity. Normalized to their TOC content, immature sources containing oil-prone Type I and II kerogens yield more hydrocarbon (higher HI) and less carbon dioxide (lower OI) than gas-prone Type III or inert Type IV kerogens. It is important to recognize that a given data point on either traditional or modified van Krevelen diagrams reflects the weighted average of all the kerogen types present in that sample, and that samples typically contain mixtures rather than consisting purely of oil-prone or gas-prone end-member kerogens (M. McCaffrey, 2008, written commun.). Peters (1986) cautioned that pyrolysis techniques commonly overestimate the liquid hydrocarbon generative potential of samples containing Type III coaly kerogen. Elemental analyses (atomic H/C and O/C ratios) and organic petrography should supplement Rock-Eval and TOC data in determining whether sufficient oil-prone kerogen is present for coals and carbonaceous shales to be effective oil source rocks (Peters, 1986). Effective oil-prone coals not only have HI in excess of 200 mg/g, but they also have atomic H/C ratio of at least 0.8–0.9 and liptinitic kerogen content of at least 15–20 percent (Hunt, 1991; Powell and Boreham, 1994; Peters and Cassa, 1994).

Langford and Blanc-Valleron (1990) argued the merits of an alternative means of kerogen characterization by applying linear regression analysis to graphs of S2 vs. TOC. There is error in the measurement of S2 due to retention of some of the pyrolyzed hydrocarbon within the rock matrix (Katz, 1983; Espitalie and others, 1985; Peters, 1986; Langford and Blanc-Valleron, 1990). The smaller the TOC, the larger this error becomes. This in turn leads to low-side bias in the calculation of hydrogen index from individual samples with low TOC, causing organically lean samples to appear to contain more gas-prone Type III kerogen than they actually do. According to Langford and Blanc-Valleron (1990), because HI is defined as S2/TOC x 100, the true average hydrogen index of a given sample population is best determined from the slope of the S2 vs. TOC regression line, not by the arithmetic mean of the individual HI values. Furthermore, the x-intercept of the regression line represents the threshold organic content required for that source rock to generate and release measurable hydrocarbon upon pyrolysis. The y-intercept directly indicates the hydrocarbon adsorption capacity, showing the amount of hydrocarbon that is retained within the source-rock matrix upon pyrolysis. Langford and Blanc-Valleron (1990) maintained that the regression approach thus provides true average HI at the same time as it corrects for and quantifies the adsorptive effect, providing a meaningful basis for distinguishing among source-rock populations that may appear very similar on traditional (H/C vs. O/C) or modified (HI vs. OI) van Krevelen diagrams.

During natural generation of oil and gas, kerogens mature (convert) into hydrocarbons across a range of temperatures, with the kerogen composition controlling the rate of generation at any given temperature. Knowledge of the thermal maturity level is critical to source-rock evaluation both for determining how much oil or gas may have been generated, and for understanding whether the measured TOC, atomic ratios, and hydrogen index correctly reflect the original generative potential. The organic carbon and pyrolyzable hydrocarbon content of high thermal maturity source rocks is reduced compared to their original (pre-maturation) values, much of it having already been spent in generating hydrocarbons. Therefore, at advanced maturity levels, even good source rocks will yield analytical results similar to poor or non-source samples.

Thermal maturity can be quantified in various ways. Rock-Eval yields a general maturity parameter $T_{max}$, the temperature (°C) at which the maximum release of pyrolyzable hydrocarbon (S2 peak) occurs during pyrolysis. More robust thermal maturity measurements can be derived from careful microscopy techniques, including vitrinite reflectance ($R_o$), thermal alteration index (TAI), and conodont alteration index (CAI). The vitrinite reflectance scale is the most widely employed in petroleum maturation studies. It measures the percentage of light reflected from vitrinite kerogen macerals. $R_o$ values are typically reported as the mean value for the in-situ vitrinite population in a given sample (excluding depositionally reworked vitrinite and any evident sample contamination). In many cases, and for the purposes of this study, a mean $R_o$ value of 0.6 percent is taken as an approximation for the onset of oil generation (for example, Peters and Cassa, 1994). Where greater precision is required, it is important to investigate reaction kinetics, which govern the transformation of kerogen to hydrocarbon in a given source rock, and varies as a function of lithology and kerogen composition.

## STRATIGRAPHIC OVERVIEW OF TRIASSIC–JURASSIC SOURCE-ROCK SUCCESSION PUALE BAY

Lower Mesozoic units of the Chignik subterrane are well exposed at the entrance and northeast shore of Puale Bay (figs. 3–5). Previous work in this area has yielded varied lithologic descriptions, and there are significant differences of opinion regarding the position and nature of formation contacts (for example, Hanson, 1957; Wang and others, 1988; Detterman and others, 1996; Wilson and others, 1999; Blodgett and Sralla, 2008). Detterman and others (1983, 1987, and 1996) were the first to extend the geographic range of the Upper Triassic Kamishak and Lower Jurassic Talkeetna formations from Cook Inlet to Puale Bay, and established a local reference section of the Lower and Middle Jurassic Kialagvik Formation there in recognition of important differences relative to the unit's type section at Wide Bay. These formations are locally faulted and gently folded, but most beds strike northeast and dip 15–30° to the northwest.

***Kamishak Formation.*** Wang and others (1988) described an approximately 700-m-thick succession at Puale Bay, consisting in ascending order of coral biomicrite, carbonate conglomerate, bedded spicular chert, and volcanic breccia. Most of this section is now assigned to the Upper Triassic Kamishak Formation, but the upper part may extend into the Lower Jurassic Talkeetna Formation as mapped by Detterman and others (1987). Detterman and others (1996) measured 800 m (2,625 ft) of Kamishak Formation in the same exposures. They described the bulk of the formation above the corralline bioclastic facies as consisting of thin- to medium-bedded gray limestones, with no mention of bedded chert.

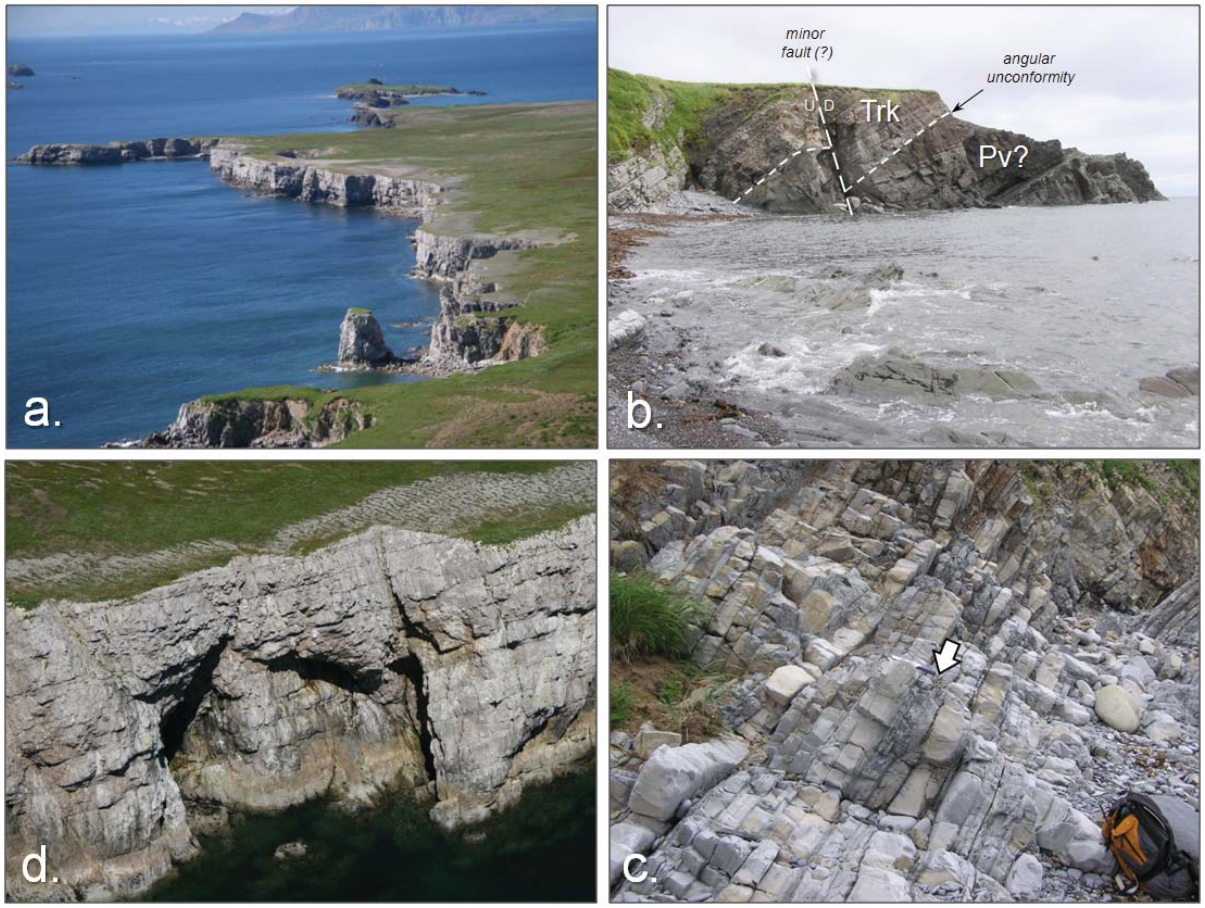


*Figure 4. Outcrop photographs of the Upper Triassic Kamishak Formation limestone near the entrance of Puale Bay. (a) View to west of lower part of formation on south-facing shoreline west of Cape Kekurnoi and east entrance to Puale Bay. (b) Angular unconformity 2.2 km west of Cape Kekurnoi; basal Kamishak overlies volcanic breccia of probable Permian age (see text for discussion). (c) Thinly laminated to medium-bedded finely crystalline limestone from lower Kamishak Formation. Sample 07PD198a, collected in the subfissile, laminated bed indicated by arrow, is an excellent oil-prone source rock (TOC = 5.28%, HI = 756 mg/g). (d) Thick-bedded bioclastic limestone facies is represented by poor to non-source lithologies, and is of more interest as potential reservoir facies.*

Observations recorded by DGGS and DOG geologists are more consistent with those of Blodgett and Sralla (2008), who describe much of the formation at Puale Bay as consisting of "thinly-bedded, dark brown to gray, argillaceous limestone and silty, calcareous shale."

Wang and others (1988) considered the base of the Triassic section to be truncated by faulting within the coral facies. Hanson (1957), Blodgett and Sralla (2008), and Blodgett (this volume) placed the base of the Triassic section farther east at an angular unconformity (fig. 4b). Blodgett and Sralla (2008) considered volcanic agglomerates immediately beneath the unconformity to be of probable Permian age due to their lithologic similarity to volcanic breccias that are apparently interbedded with Middle Permian limestones (Hanson, 1957) on small islands near the entrance to Puale Bay. Detterman and others (1987; 1996, fig. 6) and Wilson and others (1999) considered the volcanic breccias to be part of the Triassic section, and extended the outcrop belt of lower Kamishak Formation still farther east to Cape Kekurnoi (fig. 3). To the northwest, the gradational upper contact of the Kamishak with the overlying Lower Jurassic volcanic and volcaniclastic deposits mapped as Talkeetna Formation (Detterman and others, 1987; 1996; Wilson and others, 1999) has been placed where clastic sediments become predominant over limestone (Detterman and others, 1996).

During the 2007 DGGS field program, Whalen and Beatty (this volume) and Blodgett (this volume) made detailed measurements and reinterpretations of parts of

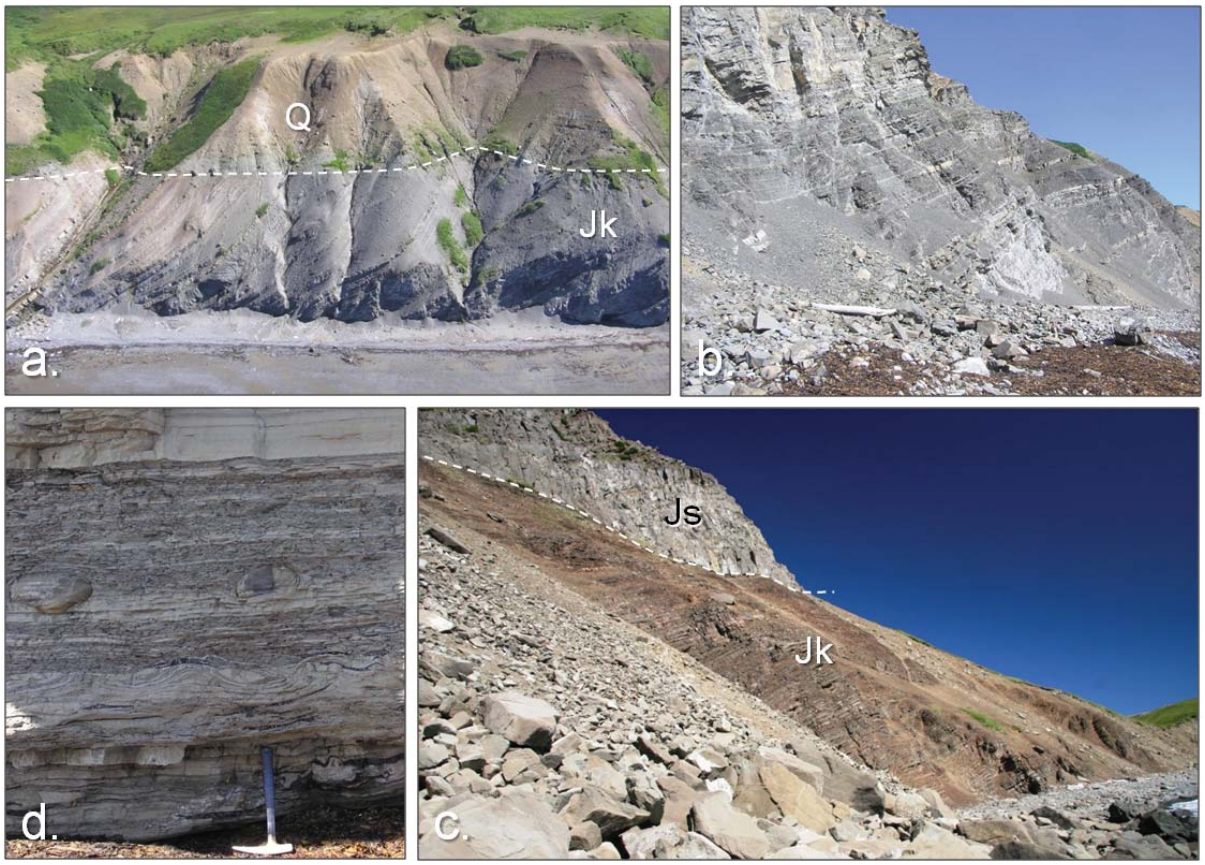


*Figure 5. Outcrop photographs of the mainly Middle Jurassic Kialagvik Formation sandstones and siltstones on the northeast shore of Puale Bay. (a) Much of the lower portion of the Kialagvik is rhythmically bedded, dark gray fissile siltstone. Quaternary unconformity (dashed line) is overlain by unconsolidated deposits (Q). (b) Generally upward-coarsening and upward-thickening succession from the middle to upper Kialagvik Formation. The finest-grained intervals consist of rhythmically bedded blocky siltstone and fine sandstone. (c) Twelve source rock samples (07RR027–038) were collected from reddish-brown weathering siliceous siltstone and sandstone interpreted here as uppermost Kialagvik (Jk) just below the contact with the overlying Shelikof Formation (Js) at the base of the cliff-forming light gray sandstone (dashed line). (d) Laminated to medium-bedded sandstones from the upper part of the section shown in photograph b contain abundant carbonaceous laminae and thin, commonly deformed coal lenses in addition to common carbonate concretions. Deposition of the middle to upper Kialagvik Formation in this area likely occurred near a deltaic sediment source, possibly under marginal marine conditions.*

the Kamishak Formation interval described by Wang and others (1988) and Detterman and others (1996). The source-rock samples discussed in this report include a number collected in these re-described intervals, but also represent other parts of the formation, including the lowermost Kamishak section farther east near the purported basal unconformity recognized by Hanson (1957) and Blodgett and Sralla (2008). The overlying Talkeetna-equivalent section was not sampled for source-rock evaluation.

***Kialagvik Formation.*** Containing megafauna ranging from late Toarcian to Callovian age (Imlay, 1984; Detterman and others, 1996), the Kialagvik Formation is largely time-equivalent to the Middle Jurassic Tuxedni Group, the source rock for most of the oils in upper Cook Inlet (Magoon and Anders, 1992). Detterman and others (1996) described the 790-m-thick Kialagvik section at Puale Bay as dominated by rhythmically interbedded siltstone and sandstone of deepwater affinity, with local intervals of massive, disorganized conglomerate. They

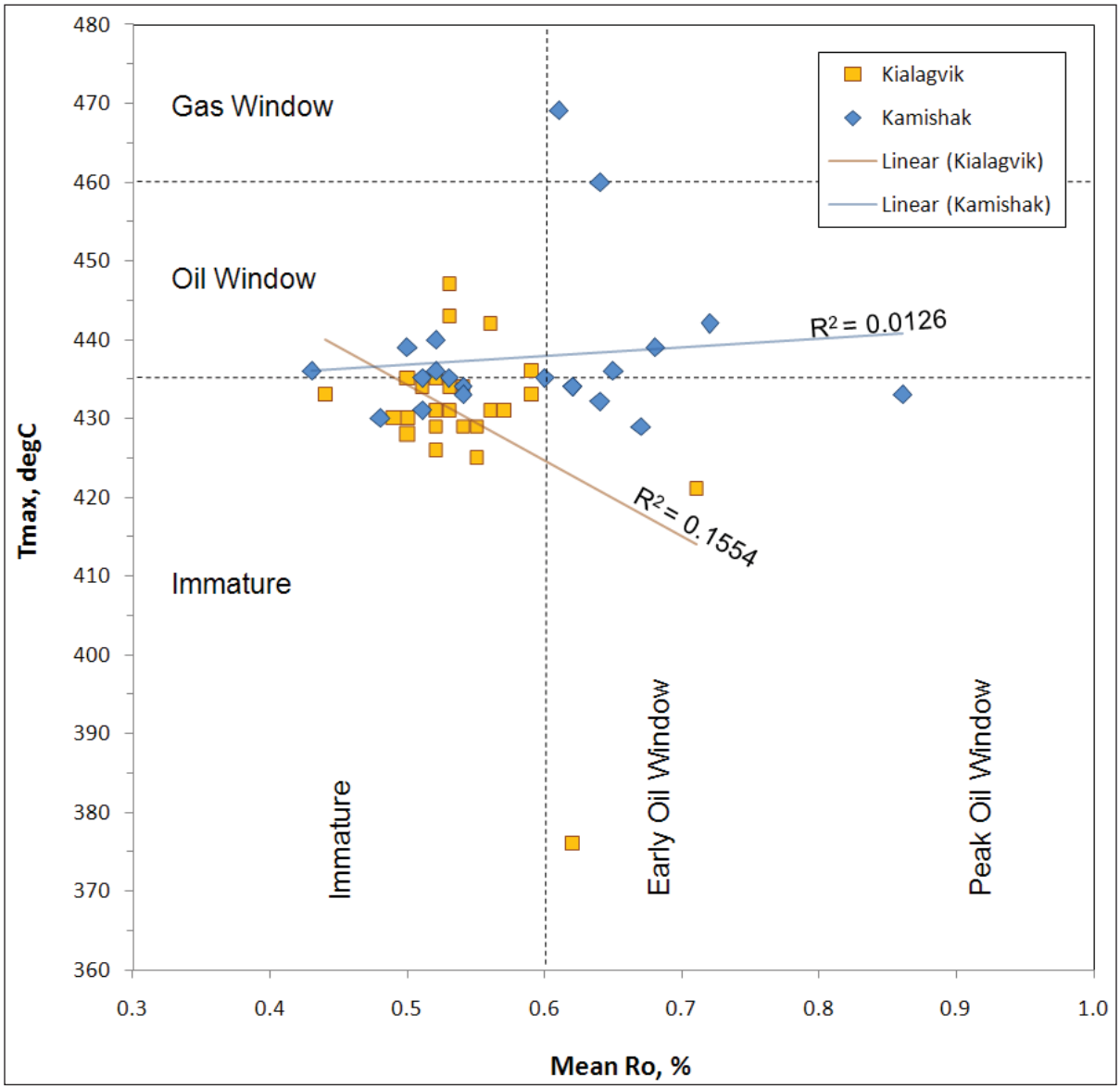


*Figure 6. Cross-plot of Rock-Eval $T_{max}$ vs. mean $R_o$ for Kamishak and Kialagvik Formation source rock samples from Puale Bay outcrops. In general, these thermal maturity parameters would be expected to show a reasonably strong positive correlation. However, the low correlation coefficient for the Kamishak regression ($R^2$ = 0.0126) indicates a weak correlation, and the negative slope of the Kialagvik regression line suggests an unlikely inverse correlation. This suggests the $T_{max}$ data should not be relied on to define the thermal maturity of individual samples. Considered as a group, and ignoring outliers, the $T_{max}$ data correctly describe the Puale Bay source rocks as mostly immature to early oil window maturity.*

noted the lithologic similarity of this section to the upper part of the unit's principal reference section at Wide Bay. In contrast, the lower part of the Wide Bay section consists of nearshore marine deposits. Significant lithology changes occur within short distances in the Kialagvik Formation, and fossils are required to make robust correlations (Imlay, 1984). The Puale Bay exposures are poorly fossiliferous relative to other exposures, leading to a lack of confident correlations between the Wide Bay and Puale Bay exposures, and with the section penetrated in the Bear Creek #1 well between the two outcrop areas (Detterman and others, 1996).

At Puale Bay, the contact with the underlying Talkeetna Formation is a conglomerate-mantled erosional unconformity. Detterman and others (1996) considered the contact with the overlying Shelikof Formation to be conformable at Puale Bay but unconformable at Wide Bay. This upper contact has been revised repeatedly, most recently by Allaway and others (1984). The formation is locally transected by subvertical dikes, and cut by steep faults with various amounts of displacement. Truncation surfaces, channel profiles, and clinoforms or lateral accretion surfaces in the rhythmically interbedded siltstones and sandstones above the massive conglomerates in the lower to middle part of the formation suggest complex deepwater depositional patterns, possibly accompanied by local slumping.

Cursory observations during geochemical sampling suggest that, with the exception of local conglomeratic packages, lithologies of the Kialagvik Formation at Puale Bay may reflect a general upward gradation to more proximal, probably shallower water deposition (fig. 5). The dark gray, fissile siltstones of the lower portion transition upward to medium to light gray, blocky siltstones and interbedded sandstones of the middle portion, where some beds contain deformed lenses of coal 0–3 cm thick. Continuing upsection, this interval becomes increasingly lighter gray with thicker carbonaceous to coaly sandstone beds. The upper part of the formation consists of reddish-gray to reddish-brown weathering, siliceous siltstone and sandstone that form steep, south-facing slopes on the northeast side of Puale Bay. It is unclear to this author whether the Kialagvik–Shelikof contact as mapped there by Detterman and others (1987) and Wilson and others (1999) is consistent with the redefinition of the contact by Allaway and others (1984) or the lithologic descriptions of this stratigraphic interval by Detterman and others (1996). Twelve samples assigned in this report to the uppermost Kialagvik Formation (07RR027a through 07RR038a) were collected in the thick, red-weathering, silicified interval at the northwestern end of the sampling traverse (fig. 5a). This interval was mapped by Detterman and others (1987) as the lowermost portion of the Shelikof Formation.

## STRATIGRAPHIC OVERVIEW OF CENOZOIC FORMATIONS, NAS COST #1 WELL

Drilled in 1982–83 to a total depth of 5,229 m (17,155 ft), the North Aleutian Shelf COST #1 well penetrated clastic strata of Eocene through Pleistocene age in the North Aleutian back-arc basin without reaching lithologic or acoustic basement (Turner and others, 1988; Mickey and others, 2005). Composed of sandstone, conglomerate, siltstone, mudstone, and coal, the well's nonmarine to shallow marine succession was initially divided into five major seismic sequences (I–V) and subdivided into 11 zones defined by lithologic, depositional, diagenetic, seismic, and petrophysical characteristics (Turner and others, 1988). More recent studies have assigned formation names to the well (Finzel and others, 2005; Sherwood and others, 2006; Decker and others, 2006). Three of the interpretive formation tops used in this report correspond to sequence-bounding seismic horizons defined by Turner and others (1988). In the absence of condensed marine shales or carbonates, the lithologies of greatest interest as potential source rocks include coals, carbonaceous mudstones, and siltstones.

***Tolstoi Formation.*** The interval from 3,164 m (10,380 ft) to the base of the well at 5,229 m (17,155 ft) measured depth in the NAS COST #1 well corresponds to seismic sequence V of Turner and others (1988). This interval is considered to be entirely Eocene in age (Mickey and others, 2005) and is assigned to the Tolstoi Formation (Sherwood and others, 2006). This thickness of more than 2,000 m (nearly 6,800 ft) represents only a partial penetration of the formation. Older strata are present in the 1,355-m-thick reference section at Ivanof Bay on the Alaska Peninsula, where the Tolstoi includes a rainforest megaflora assemblage of Late Paleocene age (Detterman and others, 1996). Interpretation of publicly available seismic data (Turner and others, 1988; Finzel and others, 2005; Sherwood and others, 2006) indicates the COST well penetrated one of several grabens that accommodated or preserved the early basin-filling sequence. In outcrop, the Tolstoi Formation varies from dominantly shallow marine strata at its type section on Pavlof Bay to progressively more nonmarine environments toward the northeast near Chignik Bay. In the well, most of the formation consists of nonmarine volcaniclastic sandstone, conglomerate, siltstone, carbonaceous mudstone, and abundant coal, with transitional marine deposits restricted to approximately the upper hundred meters (Turner and others, 1988). The base and top of the formation are unconformable onshore (Detterman and others, 1996), and probably also offshore (Worrall, 1991). Two abrupt lithologic breaks are present in the lower part of the Tolstoi interval drilled in the COST well (seismic horizons E and F). Turner and others (1988)

interpreted these surfaces as possible unconformities, presumably generated by drops in relative sea level associated with the basin's early faulting history. Sherwood and others (2006) have reinterpreted at least one of these breaks as a fault with significant stratigraphic separation.

***Stepovak, Bear Lake, and Milky River Formations.*** The Late Eocene through Pliocene interval of the NAS COST #1 well records an overall trend toward increasingly marine conditions (Turner and others, 1988, fig. 90). The Eocene to Oligocene Stepovak Formation is here assigned to the interval from 1,730 to 3,164 m (5,675 to 10,380 ft) measured depth, corresponding to seismic sequences III and IV of Turner and others (1988). Their seismic sequence II between 765 and 1,730 m (2,510 and 5,675 ft) measured depth, which probably spans late Oligocene to late Miocene time (Turner and others, 1988; Mickey and others, 2005), is interpreted as a relatively continuous offshore depositional record of the depositional cycles represented onshore by the Unga sandstone and Bear Lake Formation.

Nonmarine fluvial–deltaic sandstone, conglomerate, finer clastics, and coals dominate the lower part of the Stepovak Formation (seismic sequence IV), whereas microfossil assemblages (Turner and others, 1988) indicate that the upper Stepovak (seismic sequence III) was deposited in inner to middle shelf environments. These conditions continued during deposition of the lower part of the Bear Lake–Unga cycle before yielding to marginal marine intertonguing of diatomaceous marine strata and lignite-bearing nonmarine to delta-plain environments during deposition of the upper Bear Lake Formation.

The unconformity separating the Bear Lake and Milky River formations shows only subtle discordance in seismic data within the backarc basin (Finzel and others, 2005, fig. 4.7), but it becomes profoundly angular in the outcrop belt northeast of Port Moller (Decker and others, 2005). Microfossils from the Pliocene Milky River Formation in the COST well (interpreted here as the interval between 476 and 765 m (1,563 and 2,510 ft) measured depth are interpreted to reflect cold water conditions with slight deepening from the middle to the outer shelf (Turner and others, 1988). Unconsolidated Quaternary glaciomarine deposits constitute the section above 476 m (1,563 ft) measured depth (Turner and others, 1988; Mickey and others, 2005).

## MESOZOIC SOURCE-ROCK CHARACTERISTICS

DGGS and DOG geologists collected 38 samples from the Kamishak Formation and 39 samples from the Kialagvik Formation for source-rock evaluation at Puale Bay during 2004, 2005, and 2007 (fig. 3). TOC, Rock-Eval, mean vitrinite reflectance, and kerogen composition data from these samples are presented in table 1. This sample suite represents various lithologies from the lower, middle, and upper parts of each unit, but time constraints prohibited achieving a uniform stratigraphic sample distribution in either formation. Most samples are not precisely positioned relative to the measured sections of Whalen and Beatty (this volume), Wang and others (1988), or Detterman and others (1996).

***Thermal maturity.*** In mapping patterns of thermal maturity on the Alaska Peninsula, Molenaar (1996) lacked outcrop vitrinite reflectance data from the Puale Bay–Wide Bay area. He described the Middle Jurassic rocks in the area as undermature ($R_o$<0.6 percent) based on reflectance data from the nearby Bear Creek 1 and Wide Bay 1 wells, and the Upper Triassic outcrop section as immature to barely mature based on Rock-Eval $T_{max}$ data (Magoon and Anders, 1992; Wang and others, 1988). Table 1 presents new outcrop vitrinite reflectance results from the Kamishak Formation (23 samples) and the Kialagvik Formation (28 samples) at Puale Bay. These samples yield mean $R_o$ values ranging from 0.43 to 0.86 percent (averaging 0.60 percent) in the Kamishak and from 0.44 to 0.71 percent (averaging 0.54 percent) in the Kialagvik. This confirms the interpretations of previous workers that overall, the Puale Bay section is at immature to early oil window thermal maturity levels. Given this low thermal maturity, the Kamishak and Kialagvik formations' source characteristics revealed by TOC and Rock-Eval analyses are believed to approximate their original generative potential, little biased by loss of organic carbon and hydrogen content that would accompany greater maturation.

Figure 6 is a cross-plot of $T_{max}$ versus mean $R_o$ for all Kamishak and Kialagvik Formation samples collected in 2007. Note that despite the normally strong positive correlation between these pyrolysis-based and microscopy-based maturity measures (for example, Peters, 1986; Peters and Cassa, 1994), the regression line for the Kamishak data has a very low correlation coefficient, and the Kialagvik regression actually has a negative slope, implying an unlikely inverse correlation. As noted by Peters (1986), $T_{max}$ is a crude and often unreliable indicator of the thermal maturity of individual samples. In this case, the poor correlation between $T_{max}$ and mean $R_o$ is driven mainly by high and low outliers in the $T_{max}$ data. Even so, the $T_{max}$ data as a whole aptly characterize the overall population as mainly immature to early oil window maturity.

Molenaar (1996) observed that, despite paleo-burial to depths estimated in excess of 4,000 m, the Triassic–Jurassic section at Puale Bay remains only early mature. He concluded that the geothermal gradient during Late Cretaceous–Paleogene maximum burial must have been significantly lower than the present-day geothermal

gradient defined by wells in the Ugashik sub-basin, where the 0.6 percent $R_o$ isograd (approximating the top of the oil window) is reached at about 3,000 m.

***Kerogen type and total organic carbon.*** Given the low thermal maturity of the Puale Bay outcrop samples, a modified van Krevelen plot is useful for considering kerogen type (fig. 7). More than half of the Kamishak samples plot near the highly oil-prone Type I and II kerogen curves, many of which yield hydrogen indices in the 700–800 mg/g range. Approximately 15 percent of the Kamishak samples appear to be oil- and gas-prone Type II–III kerogen mixtures, and about one-third appear to contain mostly gas-prone Type III kerogen, including several highly oxidized samples (oxygen indices above 200 mg/g) that are off-scale, and not shown on the plot.

Organic petrography analysis of 20 Kamishak Formation samples documents the relative abundance of oil-prone liptinite, gas-prone vitrinite, and inert kerogen types. Liptinitic kerogen is overwhelmingly dominant, averaging 85 percent of the organic matter, and representing 90–95 percent in approximately two-thirds of the samples analyzed (table 1). Vitrinite makes up an average of 8 percent and inert kerogen an average of 7 percent. Samples from the coral-rich bioclastic facies contained the highest proportions of vitrinite (up to 25 percent), and inert kerogen (up to 30 percent) and the lowest proportion of liptinite (55–65 percent). These results are broadly consistent with the pyrolysis-based kerogen determinations for the Kamishak illustrated by figure 7.

Kialagvik Formation pyrolysis data (fig. 7) suggest that its overall kerogen composition is only slightly less oil-prone than that of the Kamishak. Nearly 30 percent of the Kialagvik samples plot near the Type I and II curves with HI values greater than 300 mg/g, reaching a maximum HI of 680 mg/g. More than one-third plot as Type II-III mixtures. The remaining one-third or so appear from figure 6 to consist of gas-prone Type III or inert Type IV kerogens.

Organic petrography analyses of 28 Kialagvik Formation samples indicate that, on average, liptinite constitutes 79 percent and vitrinite represents 19 percent of the organic matter, with the remaining 2 percent being inert kerogen (table 1). Liptinite makes up 90 percent or more of the kerogen in approximately two-thirds of the samples. Vitrinite constitutes 55–90 percent of the kerogen in one-fourth of the samples. These are siltstones

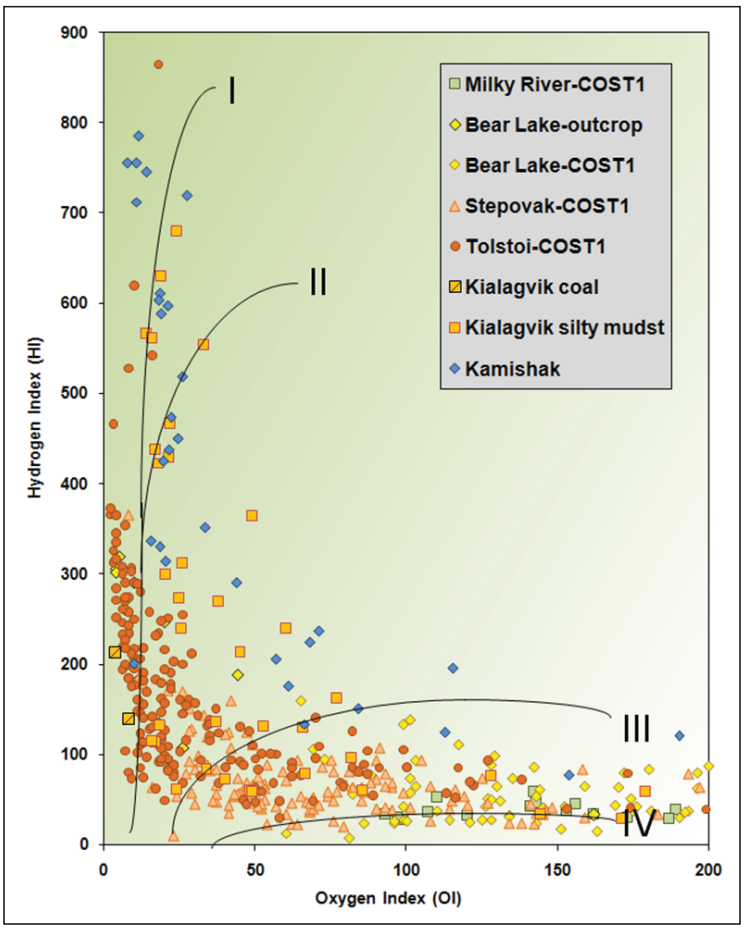


*Figure 7. Modified van Krevelen diagram, showing kerogen type determination from Rock-Eval pyrolysis data. See text for caveats of typing kerogens from coaly strata using this approach.*

and a thin coal from exposures near the middle of the formation. These Kialagvik organic petrography results are broadly consistent with the kerogen type determinations inferred from the pyrolysis data. However, many of the samples with very high liptinite:vitrinite ratios do not have correspondingly high HI values associated with good Type I and II source rocks.

Figure 8 is a graph of hydrogen index vs. total organic carbon, an effective means of screening source-rock samples for both the quantity and type of organic matter present. The colored fields in the background are loosely defined and non-unique, but they suggest the hydrocarbon products that would be expected to generate from samples as they mature. They also reflect a suite of interrelated characteristics including kerogen type, lithology, depositional environment, and thermal maturity. Both TOC and HI decrease with increasing maturity as described above, so the fields would not accurately reflect the original characteristics of highly mature source rocks. The data show a strong correlation between TOC and HI, with samples richer in organic content appearing to consist of the more oil-prone kerogens. However, Langford and Blanc-Valleron (1990) cautioned that pyrolysis experiments systematically under-predict the S2 (and thus HI) values of low-TOC samples. This is due largely to matrix adsorption effects, discussed in the subsequent section.

Considering the uncorrected pyrolysis results at face value, fully half of the Kamishak Formation limestones plot as good to excellent oil source rocks with TOC values in the 1–5 percent range and HI values greater than 300 mg/g. A few Kamishak samples fall in the lean oil or gas source categories, and about one-third contain less than 0.5 percent TOC, probably too lean to consider source-prone. These correspond to the one-third of samples that are typed as Type III kerogen from the modified van Krevelen plot (fig. 7), marked by low HI and elevated OI.

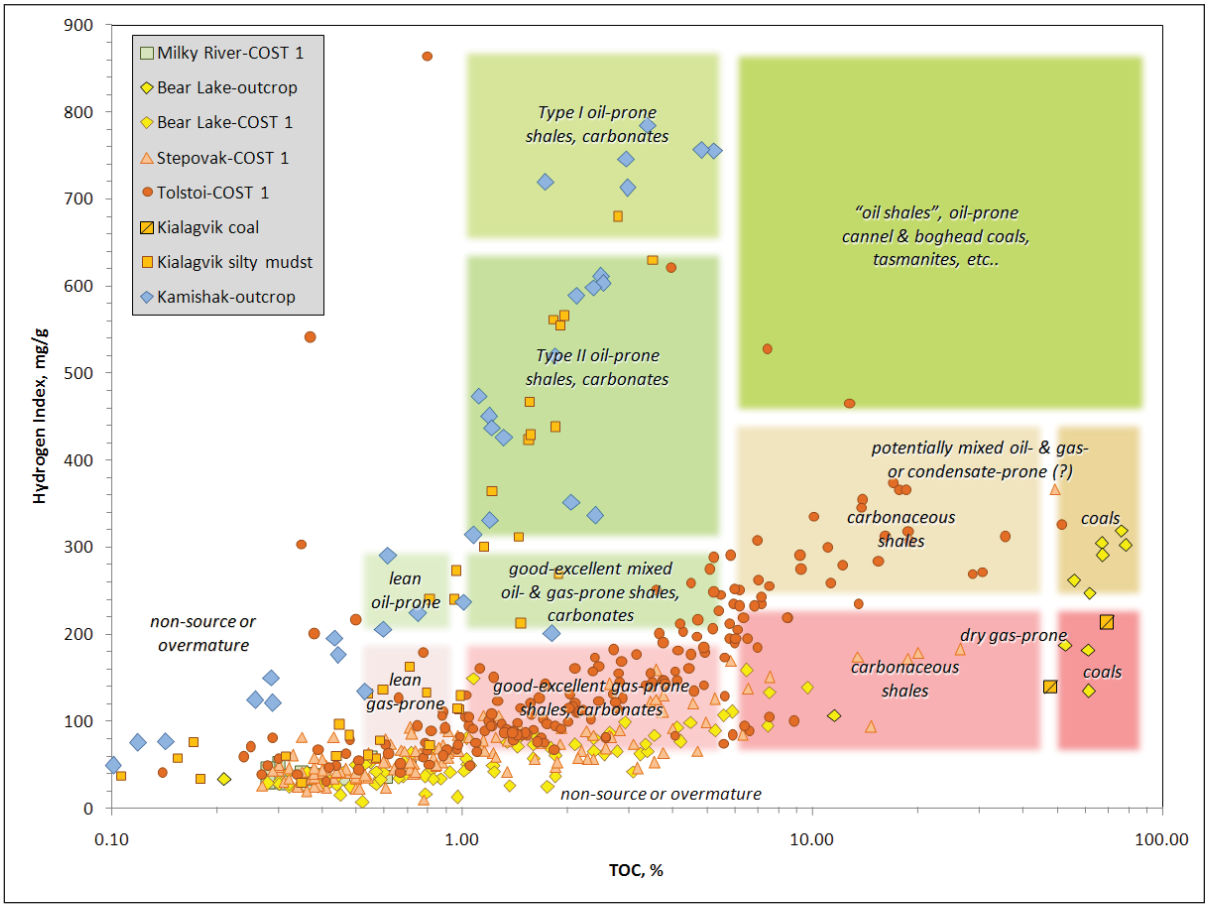


*Figure 8. Both the quantity and type of organic matter are readily apparent in a plot of hydrogen index (HI) versus total organic carbon (TOC). Samples are plotted on loosely defined fields that suggest expected hydrocarbon products and reflect other characteristics such as kerogen type, lithology, depositional environment, and maturity. These fields are non-unique, and should be considered in light of other available information, particularly in the case of coals and other rocks containing coaly kerogens.*

The silty mudstones of the Kialagvik Formation follow a trend similar to the Kamishak samples on the plot of HI vs. TOC (fig. 8). More than one-third of the Kialagvik mudstones have good to excellent TOC values in the 1–4 percent range; most of these have HI values in the range associated with oil-prone Type II kerogen (300–650 mg/g). Nearly 15 percent of Kialagvik mudstones rank a step lower in terms of source-rock quality. With TOC values in the 0.8–2 percent range and HI values ranging from 200–300 mg/g, these samples would likely generate gas-oil mixtures. Almost 20 percent of the Kialagvik mudstones plot as lean to fair gas source rocks, and about 30 percent rank here as nonviable hydrocarbon sources. Nonviable source rocks may be too lean in organic matter, thermally overmature, contain too much inert kerogen, or have high matrix adsorption capacity. Two coaly Kialagvik samples are clearly differentiated from the Kialagvik mudstones in figure 8 by their high TOC values (48 and 70 percent). Considering their moderate HI values (<215 mg/g) and high vitrinite content (90 percent in sample 07PD183B), the thin lenses of coal observed in outcrop in the middle part of the Kialagvik Formation are expected to contribute mainly dry gas. Because of their low OI values (<10 mg/g), these coals plot misleadingly in the lower-left part of the modified van Krevelen diagram (fig. 7), an area normally associated with high-maturity sources. This illustrates the point made by Peters (1986) that pyrolysis data often fail to characterize coaly sources correctly.

***Average hydrogen index and hydrocarbon adsorption capacity.*** Figure 9 presents graphs of pyrolyzable hydrocarbon (S2) versus TOC, in which source-rock sample populations plot in distinct linear trends suited to regression analysis (Langford and Blanc-Valleron, 1990). Figure 9a plots the entire data range for Mesozoic and Cenozoic samples, including coals and carbonaceous shales; figure 9b plots a more restricted data range (TOC<20 percent, S2<50 mg/g) necessary to resolve the bulk of the samples and to analyze the differences in their regression lines.

The Kamishak regression line has the steepest slope, corresponding to a "true average" HI (in the sense of Langford and Blanc-Valleron; 1990) of 745 mg/g, suggesting a strong predominance of Type I kerogen in the formation. This is substantially higher than the arithmetic average of the individual HI values, which was calculated at 359 mg/g for the same population of samples. This is presumably because of the adsorption of much of the pyrolyzed hydrocarbon from low TOC samples. The regression for the Kialagvik mudstones has a slightly lower slope that indicates an average HI of 654 mg/g. This falls near the Type I–II boundary, and is also much higher than the corresponding arithmetic mean HI of 235 mg/g. The y-intercepts of these regressions indicate the Kamishak limestones have an adsorptive capacity of 2.663 mg of pyrolyzable hydrocarbon per gram of source rock, compared to 3.145 mg/g for the Kialagvik mudstones, consistent with the observation of Langford and Blanc-Valleron (1990) that clay matrix is more adsorptive than carbonate matrix.

***Mesozoic source facies summary and stratigraphic relationships.*** Figure 10 summarizes TOC, HI, and mean $R_o$ variations in the stratigraphic succession at Puale Bay. Because the samples are not tied to a complete measured section, these three parameters are plotted here as a function of longitude. This serves as a proxy for relative stratigraphic position, since the samples are from a generally northwest-dipping succession. Sampling gaps are clearly evident in this plot, as they are on the map (fig. 3), particularly in the Kamishak Formation. Although the data are not uniformly distributed, the Kamishak data reveal multiple, high-frequency fluctuations in source-rock richness and apparent kerogen type.

The highest-quality source rocks from the Kamishak Formation represent a range of limestone lithologies. They were described in outcrop as light to medium gray or tan weathering, medium to dark gray, brown, or black fresh, micritic to finely crystalline, subfissile to blocky, planar- and ripple-laminated to medium bedded, argillaceous, fossiliferous to coquinoid limestone, typically with fetid odor. The bioclastic and adjacent knobby-weathering, nodular limestone facies include marginally gas-prone to non-source lithologies. The new organic carbon content and pyrolysis data from the Kamishak Formation agree relatively well with the results from 41 samples analyzed by Wang and others (1988, fig. 4). That paper does not present tabular data, but graphs indicate that approximately half of the samples from that study exceeded 1 percent TOC, and at least 80 percent of the samples were identified as consisting of Type I or II kerogen.

The Kialagvik TOC and HI data suggest a more systematic trend of upward-decreasing source-rock quality, with rich oil-prone facies (fissile, dark gray siltstones) in the lower part of the unit giving way to leaner gas-prone facies (blocky medium gray siltstones) in the middle, and highly variable oxidized and silicified lithologies at the top dominated by non-source and gas-prone samples. Liptinitic kerogen makes up 90 percent or more of the organic matter in all nine of the samples analyzed by organic petrography from the lower part of the formation, whereas vitrinite accounts for 55–90 percent of the kerogen from the seven samples analyzed near the middle part of the formation. This pattern is consistent with the possible upward-coarsening and/or shoaling trend noted in observations of the Kialagvik Formation at this locality. Interestingly, liptinite is the dominant kerogen type in the uppermost part of the formation, but the source-rock quality of this interval appears limited due to low total organic content, high adsorptive capacity, perhaps compounded by diagenetic alteration.

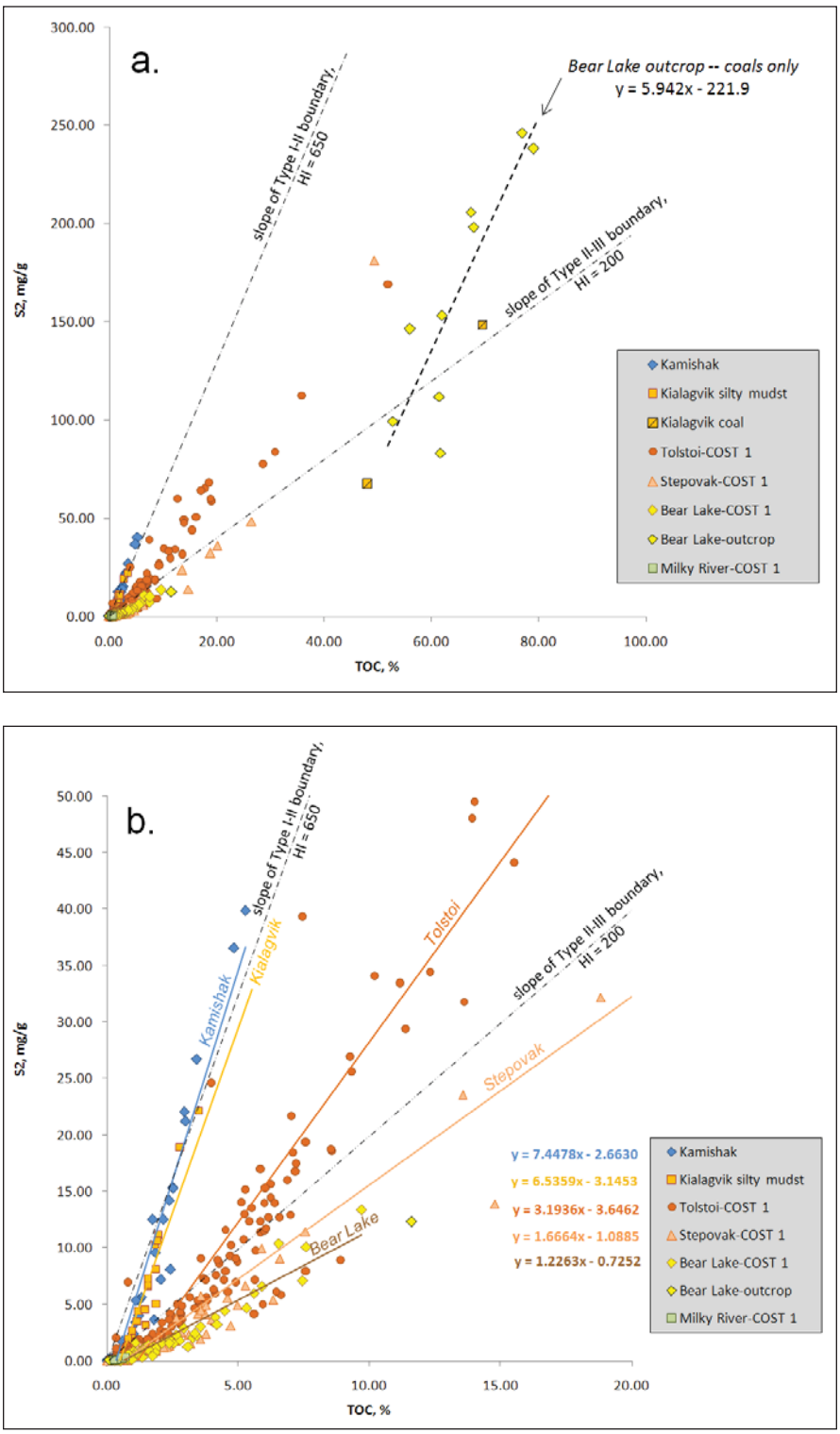


*Figure 9. Graphs of hydrolyzed hydrocarbon (S2) versus total organic carbon (TOC), following the analytical logic of Langford and Blanc-Valleron (1990). Stratigraphic order in legend is inverted to maximize visibility of all data series on plot. (a) Full data range, including coals and highly carbonaceous mudstones. See text for discussion of interpretations of regression through Bear Lake outcrop coals. (b) Restricted data range, for resolution of populations with TOC < 20% and S2 < 50 mg/g. Linear regression equations determine true average HI (slope x 100) and hydrocarbon adsorptive capacity (y-intercept) of each sample population. Type I–II boundary shown corresponds to HI = 650 (slope = 6.5), a compromise between the boundary values suggested by Langford and Blanc-Valleron (1990) and Peters and Cassa (1994).*

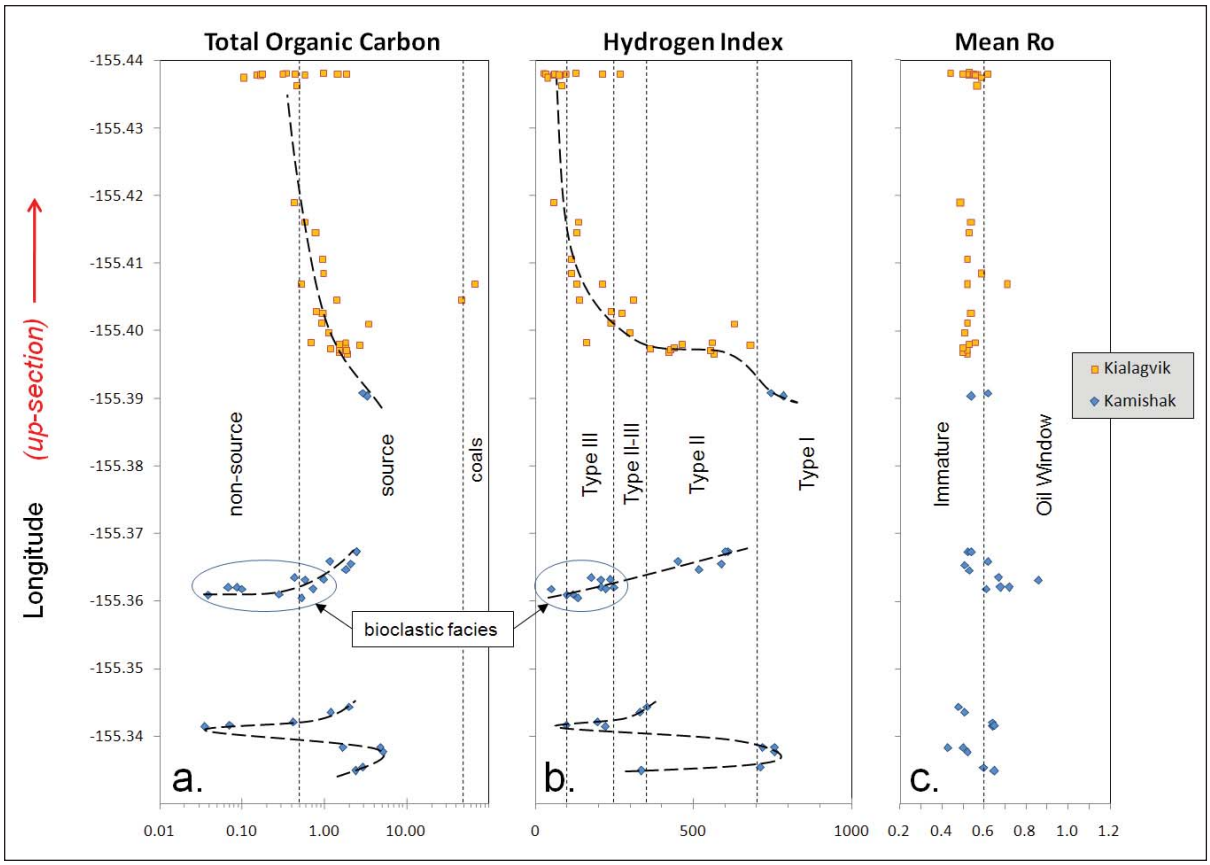


*Figure 10. TOC, HI, and mean $R_o$ of Kamishak and Kialagvik Formation samples from Puale Bay. Samples are plotted as a function of longitude, a proxy for relative stratigraphic position since these samples are from a generally northwest-dipping succession. The relationship to stratigraphic thickness is variable, depending on local fluctuations in dip magnitude and direction. Detterman and others (1996) report a 404-m-thick section of Lower Jurassic Talkeetna Formation strata between the Kamishak and Kialagvik Formations at this location. Dashed black curves are highly smoothed, visually-fit trends through the TOC and HI data, reflecting relatively high-frequency fluctuations in organic richness and apparent kerogen type throughout Kamishak deposition, versus a more systematic upward trend of decreasing source rock quality in the Kialagvik Formation. Vitrinite reflectance values average 0.60 in the Kamishak Formation and 0.54 in the Kialagvik Formation. These marginal maturity values indicate that the TOC and HI data approximate the original generative potential, with little bias attributable to transformation of organic matter to hydrocarbon.*

## CENOZOIC SOURCE-ROCK CHARACTERISTICS

Most of the Tertiary samples considered here are from the NAS COST #1 well, where more than 420 TOC and Rock-Eval analyses and 120 elemental analyses (Sherwood and others, 2006, Appendix 2) represent the Tolstoi, Stepovak, Bear Lake (including the possible Unga-equivalent interval), and Milky River Formations. Previous analyses of the well data (Dow, 1983; Turner and others, 1988; Sherwood and others, 2006) have reached many of the same conclusions supported by this report, clearly demonstrating the Tertiary section of the North Aleutian basin to be predominantly gas-prone. Nonetheless, many of these well data are presented here to facilitate direct comparison with the data from the Mesozoic outcrops at Puale Bay. Results from 12 additional Bear Lake Formation outcrop samples collected by DGGS geologists during 2004 and 2005, nine of which are coals with more than 50 percent TOC, are plotted as a discrete data series on the graphs of figures 7–9, distinct from the Bear Lake samples from the well. Populations of outcrop samples collected by DGGS workers from other Tertiary units are probably too small to stand alone as the basis of meaningful observations, and are omitted from this discussion in favor of examining the larger datasets available from the well. As in the preceding section, thermal maturity is considered first because of its impact on the interpretation of other source characteristics.

***Thermal maturity.*** Figure 11 is a plot of vitrinite reflectance vs. depth from the NAS COST #1 well, showing a well-defined linear maturity gradient. A significant offset in the profile at 761 m (15,620 ft) measured depth in the Tolstoi Formation is attributable either to erosion at an intra-formational unconformity or omission of section by normal faulting (Sherwood and others, 2006, fig. 17). Based on this gradient, the main oil generation window (0.6 to 1.35 percent $R_o$) extends from approximately -3,750 m (-12,300 ft) subsea (~3,780 m/~12,400 ft measured depth) to about -5,640 m (-18,500 ft) subsea, below the well's total depth. Thus, while much of the Tolstoi Formation is mature for hydrocarbon generation at this location, the overlying Stepovak, Bear Lake, and Milky River Formations are all thermally immature. Only the deeper parts of the Tolstoi Formation may have originally had significantly more organic carbon and hydrogen content (more oil-generating potential) than their TOC and Rock-Eval measurements described below would indicate. Substantial gas generation is expected to have occurred from carbonaceous and coaly source intervals that are at oil window or greater maturity in the middle and lower portions of the Tolstoi Formation (Boreham and Powell, 1993; Sherwood and others, 2006). Ongoing dry gas generation is expected within the lowest part of the sedimentary section in this graben. Burial history modeling (Sherwood and others, 2006, fig. 30) estimates that Tolstoi strata at the floor of the graben entered the main oil window during latest Eocene or earliest Oligocene time (~34 Ma), and passed into the main gas generation window during latest Oligocene time (~24 Ma).

Sherwood and others (2006) described complications in defining a single geothermal gradient that is appropriate for the entire NAS COST #1 well. Their burial history modeling suggested a geothermal gradient of 30.4 to 31.0°C/km (1.67 to 1.7°F/1,000 ft) for the interval below ~1,500 m (4,900 ft) measured depth. This is virtually identical to the 31°C/km gradient calculated for the well as a whole by Turner and others (1988) and Bergman, Murphy, and Kelley (this volume). Molenaar (1996) derived somewhat higher present-day geothermal gradients from onshore wells, averaging 34.6°C/km near the edge of the backarc basin onshore in the Bristol Bay Lowlands, and averaging 36.5°C/km in the volcanic arc and outcrop belt. Seismic, biostratigraphic, and fission-track data (Turner and others, 1988; Sherwood and others, 2006; Bergman, Murphy, and Kelley, this volume) support the interpretation that the backarc basin, and in particular the graben drilled by the COST well, has experienced a simple subsidence history, reaching maximum temperatures in the recent past.

***Kerogen type and total organic carbon.*** Taken at face value without regard to the previously discussed caveats about using pyrolysis techniques for kerogen characterization in coaly organic matter, the modified van Krevelen plot (fig. 7) would suggest that the Cenozoic samples include a wide range of kerogen macerals,

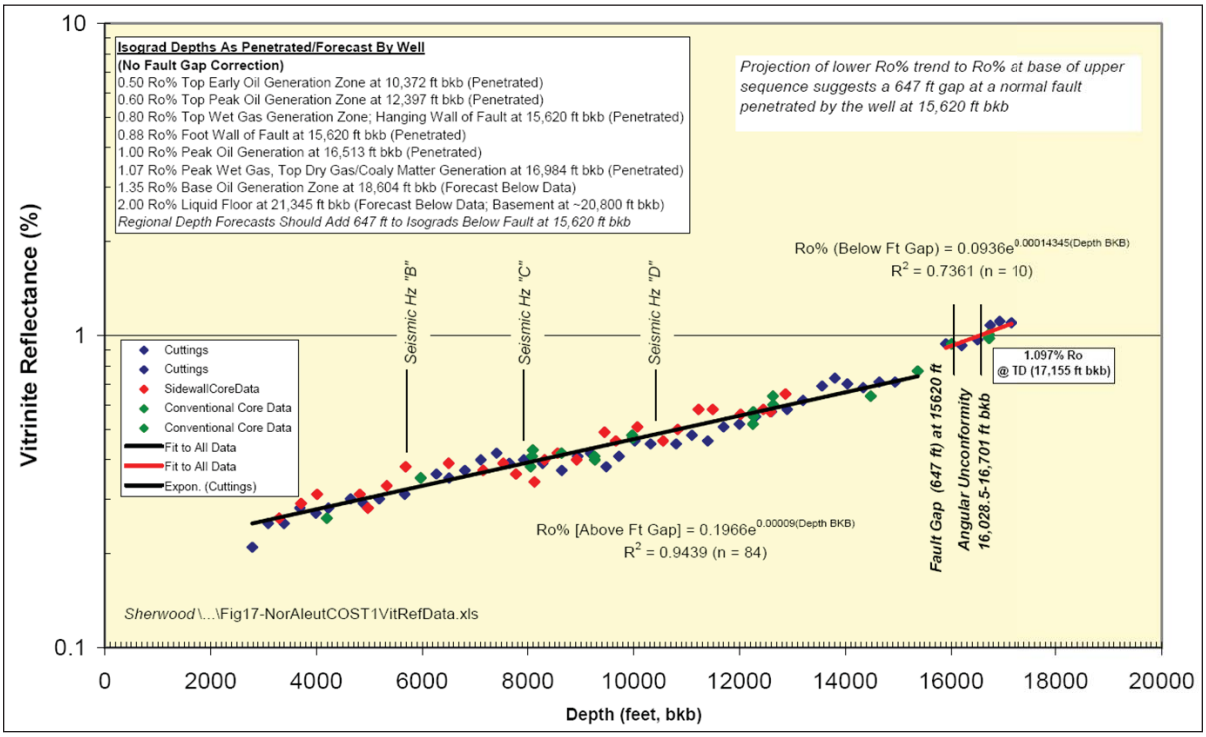


*Figure 11. Vitrinite reflectance profile for NAS COST 1 well from Sherwood and others, 2006.*

including inert (Type IV), gas-prone (Type III), and possibly liquid-prone (Type I–II and II–III) forms. Given the shallow marine to nonmarine depositional setting in the North Aleutian basin, it is not surprising that many of the well samples, including nearly all from the Stepovak, Bear Lake, and Milky River Formations appear to consist mostly of gas-prone or inert kerogens. However, there is a large number of Tolstoi Formation samples and a small group of coals from the Bear Lake outcrop belt that have elevated HI values (>200 mg/g) and low OI values (<25 mg/g). These merit further discussion as to whether they should be considered potential liquid-prone source rocks, particularly those with HI in excess of 300 mg/g. Most of the Tolstoi samples with HI values above 200 mg/g are from between 3,660 and 4,785 m (12,000 and 15,700 ft) measured depth (Sherwood and others, 2006, fig. 21).

Kerogen typing from organic microscopy in the NAS COST #1 well (Turner and others, 1988, fig. 93) indicates that much of the Tolstoi interval with HI in excess of 200 mg/g also contains 15–25 percent liptinitic kerogen as a mix of amorphous (Type I algal, sapropelic or structureless) and exinite (Type I–II structured herbaceous, lipid-rich) macerals. Atomic ratio data are also available for a subset of the samples from the well (Dow, 1983; Sherwood and others, 2006). Most of the samples with HI values greater than 200 mg/g that were also analyzed for elemental composition have H/C ratios between 0.8 and 1.0. Considered together, their HI, petrographic characteristics, and elemental compositions place these Tolstoi samples in the marginal range for oil expulsion (Hunt, 1991; Powell and Boreham, 1994; Peters and Cassa, 1994), albeit near the Type III curve on a true van Krevelen diagram (Sherwood and others, 2006, fig. 22).

The HI vs. TOC plot (fig. 8) suggests correctly that the Tertiary succession consists of a mix of lithologies, including non-source sandstones and siltstones as well as source-prone mudstones, carbonaceous shales (~6–50 percent TOC), and true coals (>50 percent TOC). There is significant overlap between samples of the Stepovak, Bear Lake, and Milky River Formations. Above about 1 percent TOC, most Tolstoi samples define a substantially higher HI trend than the younger formations (fig. 9b). All but a few of the Tertiary samples with HI>200 mg/g also have TOC values above 3–4 percent; those with HI ranging 300 to 400 mg/g are mostly carbonaceous shales of the Tolstoi Formation and a few of the coals from the Bear Lake outcrop belt. Several Tolstoi samples have HI greater than 450 mg/g paired with widely scattered TOC values; a few with TOC elevated above 4 percent could potentially represent either restricted marine or lacustrine shales (fig. 8). The high HI values of those with low TOC values may result from spuriously low TOC measurements, since HI is defined by the S2/TOC ratio. These exceptions and caveats notwithstanding, the distinctly higher HI vs. TOC trend of the main Tolstoi population relative to most samples from the other Tertiary formations is noteworthy.

***Average hydrogen index and hydrocarbon adsorption capacity.*** S2 vs. TOC regression lines for the Tolstoi, Stepovak, and Bear Lake sample populations from the NAS COST #1 well are shown on the graph of figure 9b. The smaller Milky River population, besides being statistically less robust, is of little consequence as a potential thermogenic or biogenic source in the North Aleutian basin (shallow burial, organically lean), and is not subjected to regression analysis. The small group of true coals from outcrops of the Bear Lake Formation is analyzed independently (non-coal outcrop samples excluded) in figure 9a.

The Tertiary sample populations cluster into relatively distinct trends in these S2 vs. TOC cross plot of figure 9b. The Tolstoi regression has the steepest slope, equating to a true average HI of 319 mg/g, consistent with a substantial Type II kerogen content. A single sidewall core sample from the lower part of the Stepovak Formation at 2,534 m (8,314 ft) measured depth plots as an outlier near the center of figure 9a (TOC=49.5 percent, S2=181 mg/g). This sample is excluded from the Stepovak regression, since it is for all practical purposes a coal, whereas the other samples represent a range of muddy to sandy clastic lithologies. The resulting regression reveals that non-coal sources of the Stepovak Formation have a true average HI of 167 mg/g. The non-coal population from the Bear Lake interval in the COST well has a still lower slope, representing a true average HI of 123 mg/g. Both of these are below the 200 mg/g HI boundary suggested as an approximate upper limit for gas-prone Type III kerogen (Langford and Blanc-Valleron, 1990; Peters and Cassa, 1994).

The regression-based true average HI values suggest that the Stepovak and Bear Lake formations would be expected to generate only dry gas, but the Tolstoi Formation could potentially generate light hydrocarbon liquids in addition to gas. Coals and coaly organic matter are now well accepted as the source of oil accumulations in Australia, Indonesia, and other areas (Clayton, 1993; Powell and Boreham, 1994; Fleet and Scott, 1994; Peters and Cassa, 1994). Multiple lines of geochemical evidence demonstrate that coals from the Eocene Kulthieth Formation may source some of the natural oil seeps in the Gulf of Alaska region (Van Kooten and others, 2002).

The limiting factor in the effectiveness of coaly strata as oil source rocks is commonly their low expulsion efficiency (Fleet and Scott, 1994), largely a function of high hydrocarbon adsorption capacity. As an illustration, consider the regression through the small dataset of coals from Bear Lake Formation outcrops (fig. 9a). Although

the steep slope of the regression indicates that these coals have a high average HI (594 mg/g) consistent with the potential for generating liquid petroleum, the regression line is shifted far to the right, with a large negative y-intercept. The adsorptive capacity of the Bear Lake outcrop coals is 222 mg of hydrocarbon per gram of source rock, nearly two orders of magnitude higher than that of the Kamishak carbonates, meaning that relatively little of the hydrocarbon generated would be expelled.

***Cenozoic source facies summary.*** Taken together, the TOC, Rock-Eval pyrolysis data, organic microscopy, atomic ratio, and thermal maturity data from the NAS COST #1 well indicate that the Tertiary succession of the North Aleutian basin contains abundant gas-prone source facies in the Tolstoi, Stepovak, and Bear Lake Formations. However, only the deeper portions of the basin below about -3,750 m (-12,300 ft) subsea are expected to have experienced significant thermogenic generation. Some coaly siltstones, carbonaceous mudstones, and shales of the Tolstoi Formation penetrated in the well between 3,660 and 4,785 m (12,000–15,700 ft) measured depth may meet the criteria (Hunt, 1991; Powell and Boreham, 1994; Peters and Cassa, 1994) for coaly sources that are at least marginally capable of generating and expelling light hydrocarbon liquids. This is in keeping with the findings of Sherwood and others (2006) that the minor oil shows from the lower part of the NAS COST #1 well yield carbon isotope values, pristane/phytane ratios, and biomarker signatures tying them to Tertiary terrigenous source facies rather than the marine source rocks of the Jurassic and Triassic units.

## DISCUSSION AND CONCLUSIONS

Despite major lithologic contrasts between the carbonate-dominated Triassic Kamishak Formation and the siliciclastic mudstones, siltstones, and sandstones of the Jurassic Kialagvik Formation, Rock-Eval, TOC, and kerogen petrography analyses indicate that both units contain highly oil-prone source facies. True average hydrogen indices (HI) in the 650–750 mg/g range determined from S2-TOC regressions reflect the strong predominance of Type I–II kerogen, consistent with liptinite contents averaging approximately 80 to 85 percent in both units, despite the local occurrence of thin vitrinitic coals in the Kialagvik Formation.

Although there is no evidence that these Mesozoic source rocks underlie substantial offshore portions of the North Aleutian basin, the outcrop distribution of Chignik subterrane units suggests they may locally source onshore and nearshore plays on acreage offered in Alaska Peninsula areawide lease sales. The importance of the Middle Jurassic Tuxedni Group (Kialagvik equivalent) as the source of commercial oil in upper Cook Inlet fields is well established from geochemical evidence (Magoon and Claypool, 1981; Magoon and Anders, 1990, 1992; Magoon, 1994), and Upper Triassic rocks (Kamishak equivalent) have been identified as a co-source of oils in lower Cook Inlet (Magoon and Anders, 1990, 1992). Future outcrop study of these Mesozoic source rocks should strive to integrate pyrolysis data with measured section thicknesses in order to quantify source potential index (Demaison and Huizinga, 1994). This parameter is valuable in constraining basin models, as it represents the maximum quantity of hydrocarbons that can be generated per square meter of a source rock unit's areal extent.

In contrast, the Cenozoic formations penetrated at the NAS COST #1 well are considerably more gas-prone, in keeping with the shallow marine to nonmarine depositional environment and corresponding predominance of terrestrially-derived coaly kerogen. Although interpreted as mostly nonmarine at this location, the Eocene Tolstoi Formation's true average hydrogen index of 319 mg/g suggests that portions of its carbonaceous shale facies with elevated liptinitic kerogen content and H:C ratio may possess marginal capability to generate petroleum liquids in addition to natural gas. Because the middle and lower parts of the Tolstoi are thermally mature for hydrocarbon generation, their original TOC and HI values (and thus liquids-generation potential) would have been somewhat higher still. However, the high adsorptive capacity associated with coaly kerogens may have limited the unit's expulsion efficiency. A small population of Miocene Bear Lake Formation coals collected in outcrop has a true average HI of nearly 600 mg/g, but their adsorptive capacity is nearly two orders of magnitude higher than those of the other units. Any liquid hydrocarbons generated are unlikely to have migrated out of these Bear Lake coals. The Bear Lake Formation and Eocene–Oligocene Stepovak Formation shales and carbonaceous shales from the COST well nearly all appear capable of generating only dry gas upon thermogenic maturation. However, at least in the deep graben penetrated by the well, the zone of thermogenic generation potential lies entirely within and below the Tolstoi Formation.

## ACKNOWLEDGMENTS

Field work and analyses for this study were conducted during 2004, 2005, and 2007 with funding from multiple sources, including a U.S. Department of Energy grant from the Arctic Energy Technology Development Laboratory at the University of Alaska Fairbanks to Rocky Reifenstuhl (program head) and Paul McCarthy (principal investigator, UAF); Bristol Bay Native Corporation; and Division of Geological & Geophysical Surveys and Division of Oil and Gas operating and capital improvement project budgets. Field samples were

collected by Rocky Reifenstuhl, Robert Gillis, Emily Finzel, and Karen Clautice (DGGS); the author, David Shafer, and Timothy Ryherd, (DOG); Michael Whalen (UAF); and Robert Blodgett (consulting geologist). The text and figures benefited greatly from insightful reviews by Mark McCaffrey and Art Banet.

## REFERENCES CITED

Allaway, W.H., Jr., Detterman, R.L, Miller, J.W., and Magoon, L.B., 1984, Stratigraphic clarification of the Shelikof Formation, Alaska Peninsula, *in* Stratigraphic notes, 1983: U.S. Geological Survey Bulletin 1537-A, p. A21-A27.

Beeman, W.R., Obuch, R.C., and Brewton, J.D., 1996, Digital map data, text, and graphical images in support of the 1995 National Assessment of United States Oil and Gas Resources: U.S. Geological Survey Digital Data Series DDS-35, 1 disk, http://pubs.usgs.gov/dds/dds-035/DDS-35.html

Beikman, H.M., 1980, Geologic map of Alaska: U.S. Geological Survey Professional Paper 171, 1 plate, scale 1:2,500,000.

Bergman, S.C., Murphy, John, and Kelley, Shari, this volume.

Blodgett, R.B., this volume.

Blodgett, R.B., and Clautice, K.H., 2005, Oil and gas seeps of the Puale Bay–Becharof Lake–Wide Bay region, northern Alaska Peninsula: Alaska Division of Geological & Geophysical Surveys Preliminary Interpretive Report 2005-6, 13 p., 1 sheet.

Blodgett, R.B., and Sralla, Bryan, 2008, A major unconformity between Permian and Triassic strata at Cape Kekurnoi, Alaska Peninsula; Old and new observations on stratigraphy and hydrocarbon potential, *in* Haeussler, P.J., and Galloway, J.P., eds., Studies by the U.S. Geological Survey in Alaska, 2006: U.S. Geological Survey Professional Paper 1739-E, 13 p. [http://pubs.usgs.gov/pp/pp1739/e/].

Boreham, C.J., and Powell, T.G., 1993; Petroleum source rock potential of coal and associated sediments—qualitative and quantitative aspects, *in* Law, B.E., and Rice, D.D., eds., Hydrocarbons from coal: American Association of Petroleum Geologists Studies in Geology 38, p. 133–157.

Clayton, J.L., 1993, Composition of crude oils generated from coals and coaly organic matter in shales, *in* Law, B.E., and Rice, D.D., eds., Hydrocarbons from coal: American Association of Petroleum Geologists Studies in Geology 38, p. 185–201.

Decker, P.L., Finzel, E.S., Ridgway, K.D., Reifenstuhl, R.R., and Blodgett, R.B., 2005, Preliminary summary of the 2005 field season; Port Moller, Herendeen Bay, and Dillingham areas, Bristol Bay Basin, Alaska Peninsula: Alaska Division of Geological & Geophysical Surveys Preliminary Interpretive Report 2005-7, 55 p., 2 sheets.

Decker, P.L., Reifenstuhl, R.R., and Gillis, R.J., this volume.

Decker, P.L., Reifenstuhl, R.R., Finzel, E.S., and Helmold, K.P., 2006, Play concepts for reopening the Bristol Bay basin; Tertiary and Mesozoic petroleum systems of the Alaska Peninsula [abs.]: American Association of Petroleum Geologists Bulletin, v. 90, Program Abstracts (digital).

Demaison, G., and Huizinga, B.J., 1994, Genetic classification of petroleum systems using three factors; Charge, migration and entrapment, *in* Magoon, L.B., and Dow, W.G., eds., The petroleum system—from source to trap: American Association of Petroleum Geologists Memoir 60, p.73–89.

Detterman, R.L., Case, J.E., Wilson, F.H., Yount, M.E., and Allaway, W.H., Jr., 1983, Generalized geologic map of the Ugashik, Bristol Bay, and part of Karluk quadrangles, Alaska: U.S. Geological Survey Miscellaneous Field Studies Map 1539-A, 1 plate, scale 1:250,000.

Detterman, R.L., Case, J.E., Wilson, F.H., and Yount, M.E., 1987, Geologic map of the Ugashik, Bristol Bay, and western part of Karluk quadrangles, Alaska: U.S. Geological Survey Miscellaneous Investigations Series Map 1685, 1 plate, scale 1:250,000.

Detterman, R.L., Case, J.E., Miller, J.W., Wilson, F.H., and Yount, M.E., 1996, Stratigraphic framework of the Alaska Peninsula: U.S. Geological Survey Bulletin 1969-A, 74 p.

Dow, W.G., 1977, Kerogen studies and geological interpretations: Journal of Geochemical Exploration, v. 7, p. 79–99.

Dow, W.G., 1983, Geochemical analysis of North Aleutian Shelf Cost No. 1 well, Alaska: Minerals Management Service public well files – Robertson Research Report No. 823/135, 315 p.

Espitalié, J., Laporte, J.L., Madec, M., Marquis, F., Leplat, P., Paulet, J., Boutefeu, A., 1977, Methode rapide de caracterisation des roches meres, de leur potential petrolier et de leur degree d'evolution: Revue de l'Institut Français du Pétrole, v. 32, p. 23–42.

Espitalié, J., Deroo, G., and Marquis, F., 1985, La pyrolyse Rock-Eval et ses applications: Revue de l'Institut Français du Pétrole, v. 40, p. 563–579 and 755–784.

Finzel, E.S., Reifenstuhl, R.R., Decker, P.L., and Ridgway, K.D., 2005, Sedimentology, stratigraphy, and hydrocarbon reservoir—source rock potential, using surface and subsurface data, of Tertiary and Mesozoic strata, Bristol Bay basin and Alaska Peninsula: Alaska Division of Geological & Geophysical Surveys Preliminary Interpretive Report 2005-4, 67 p.

Fleet, A.J., and Scott, A.C., 1994, Coal and coal-bearing strata as oil-prone source rocks; An overview, *in* Scott, A.C., and Fleet, A.J., eds., Coal and coal-bearing strata as oil-prone source rocks?: Geological Society Special Publication No. 77, p. 1–8.

Hanson, B.M., 1957, Middle Permian limestone on Pacific side of Alaska Peninsula: American Association of Petroleum Geologists Bulletin, v. 41, no. 10, p. 2,376–2,378.

Hunt, J.M., 1991, Generation of gas and oil from coal and other terrestrial organic matter: Organic Geochemistry, v. 17, p. 673–680.

Imlay, R.W., 1984, Early and middle Bajocian (Middle Jurassic) ammonites from southern Alaska: U.S. Geological Survey Professional Paper 1322, 38 p., 2 plates.

Katz, B.J., 1983, Limitations of 'Rock-Eval' pyrolysis for typing organic matter: Organic Geochemistry, v. 4, p. 195–199.

Kirschner, C.L., 1988, Map showing sedimentary basins of offshore and continental shelf areas, Alaska: U.S. Geological Survey Miscellaneous Investigations Series 1873, 1 plate, scale 1:2,500,000.

Langford, F.F., and Blanc-Valleron, M.-M., 1990, Interpreting Rock-Eval pyrolysis data using graphs of pyrolyzable hydrocarbons vs. total organic carbon: American Association of Petroleum Geologists Bulletin, v. 74, p. 799–804.

Magoon, L.B., 1994, Tuxedni–Hemlock(!) petroleum system in Cook Inlet, Alaska, U.S.A., *in* Magoon, L.B., and Dow, W.G., eds., The petroleum system—from source to trap: American Association of Petroleum Geologists Memoir 60, p. 359–370.

Magoon, L.B., and Anders, D.E., 1990, Oil-source rock correlation using carbon isotope data and biological marker compounds, Cook Inlet-Alaska Peninsula [abs.]: American Association of Petroleum Geologists Bulletin, v. 74, p. 711.

Magoon, L.B., and Anders, D.E., 1992, Oil-to-source rock correlation using carbon–isotopic data and biological marker compounds, Cook Inlet–Alaska Peninsula, Alaska, *in* Moldowan, J.M., Albrecht, P., and Philip, R.P., eds., Biological Markers in Sediments and Petroleum: Prentice Hall, Englewood Cliffs, New Jersey, p. 241–274.

Magoon, L.B., and Claypool, G.E., 1981, Petroleum geology of Cook Inlet basin; an exploration model: American Association of Petroleum Geologists Bulletin, v. 65, p. 1,043–1,061.

Mickey, M.B., Haga, H. Boettcher, R.S., and Kling, S.A., 2005, Northwestern Alaska Peninsula–Bristol Bay basin biostratigraphy study: Micropaleo Consultants Job No. 25-104, 287 p., 4 oversize plates, 40 oversize figures, Alaska Division of Oil & Gas online publication http://www.dog.dnr.state.ak.us/oil/products/publications/akpeninsula/biostrat.htm

Molenaar, C.M., 1996, Thermal-maturity patterns and geothermal gradients on the Alaska Peninsula, *in* Johnsson, M.J., and Howell, D.G., eds., Thermal evolution of sedimentary basins in Alaska: U.S. Geological Survey Bulletin 2142, p. 11–19.

Peters, K.E., 1986, Guidelines for evaluating petroleum source rock using programmed pyrolysis: American Association of Petroleum Geologists Bulletin, v. 70, p. 318–329.

Peters, K.E., and Cassa, M.R., 1994, Applied source rock geochemistry, *in* Magoon, L.B., and Dow, W.G., eds., The petroleum system—from source to trap: American Association of Petroleum Geologists Memoir 60, p. 93–117.

Powell, T.G., and Boreham, C.J., 1994, Terrestrially sourced oils; Where do they exist and what are our limits of knowledge? – A geochemical perspective, *in* Scott, A.C., and Fleet, A.J., eds., Coal and coal-bearing strata as oil-prone source rocks?: Geological Society Special Publication No. 77, p. 11–29.

Reifenstuhl, R.R., Decker, P.L., Gillis, R.J., Helmold, K.P., and Strauch, A., 2007, Hydrocarbon systems, basin analyses, and 2006 field and subsurface data; Bristol Bay, Alaska Peninsula, Frontier Basin [abs.]: American Association of Petroleum Geologists Bulletin, v. 91, Program Abstracts (digital).

Sherwood, K.W., Larson, J., Comer, C.D., Craig, J.D., and Reitmeier, C., 2006, North Aleutian basin OCS planning area assessment of undiscovered technically-recoverable oil and gas: U.S. Minerals Management Service Alaska OCS Region report, 138 p., 4 plates, www.mms.gov/alaska/re/reports/rereport.htm.

Tissot, B.P., and Welte, D.H., 1984, Petroleum formation and occurrence, 2nd ed.: Berlin, Springer-Verlag, 699 p.

Turner, R.F., McCarthy, C.M., Lynch, M.B., Hoose, P.J., Martin, G.C., Larson, J.A., Flett, T.O., Sherwood, K.W., and Adams, A.J., 1988, Geological and operational summary, North Aleutian Shelf COST No. 1 well, Bering Sea, Alaska: Minerals Management Service, Alaska OCS Region, OCS Report MMS 88-089, 256 p., 2 plates.

Van Kooten, G.K., Short, J.W., and Kolak, J.J., 2002, Low-maturity Kulthieth Formation coal; A possible source of the polycyclic aromatic hydrocarbons in benthic sediments of the northern Gulf of Alaska: Environmental Forensics, v. 3, p. 227–241.

Wang, Jason, Newton, C.R., and Dunne, L., 1988, Late Triassic transition from biogenic to arc sedimentation on the Peninsular terrane, Puale Bay, Alaska Peninsula: Geological Society of America Bulletin, v. 100, no. 9, p. 1,466–1,478.

Whalen, M., this volume.

Wilson, F.H., Detterman, R.L., and Case, J.E., 1985, The Alaska Peninsula terrane; A definition: U.S. Geological Survey Open-File Report 85-450, 17 p.

Wilson, F.H., Detterman, R.L., and DuBois, Gregory, 1999, Digital data for the geologic framework of the Alaska Peninsula, Southwest Alaska, and the Alaska Peninsula Terrane: U.S. Geological Survey Open-File Report 99-317, 41 p., 1 plate, http://wrgis.wr.usgs.gov/open-file/of99-317.

Worrall, D.M., 1991, Tectonic history of the Bering Sea and the evolution of Tertiary strike-slip basins of the Bering Shelf: Geological Society of America Special Paper 257, 120 p., 1 oversize sheet, 4 plates.